universität wien

MASTERARBEIT / MASTER'S THESIS

Titel der Masterarbeit / Title of the Master's Thesis

„A new piercing proboscis? Comparison of the feeding apparatus of *Acherontia atropos* and *Agrius convolvuli* (Lepidoptera)"

verfasst von / submitted by

Caroline Reinwald, BSc

angestrebter akademischer Grad / in partial fulfilment of the requirements for the degree of
Master of Science (MSc)

Wien, 2021 / Vienna, 2021

Studienkennzahl lt. Studienblatt / degree programme code as it appears on the student record sheet:	A 066 831
Studienrichtung lt. Studienblatt / degree programme as it appears on the student record sheet:	Masterstudium Zoologie
Betreut von / Supervisor:	ao. Univ. Prof. Mag. Dr. Harald W. Krenn

Acknowledgements

I would like to thank my supervisor, Univ. Prof. Mag. Dr. Harald W. Krenn, for always taking time for me, for providing me with decades of profound knowledge and for truly making me feel like a part of the department. But also, for being a driving force since my first zoology lecture as a bachelor student and for motivating and inspiring me to continue down this path.

Furthermore, I wanted to express my gratitude to Julia Bauder, PhD, who provided me with the semithin sections of the analyzed specimens and has taught me some of the fundamental methods of my work. I also want to thank her for cheering me on throughout the entire process.

Additionally, I want to thank Brian Metscher, Bsc. PhD, who performed the microCT-scans I worked with and provided me with the basic skills for working with the software Amira.

Finally, I want to thank my family for always supporting my dream of becoming a biologist, even way back when I was a child. I am forever grateful to be surrounded by such amazing and caring people, because without them, I wouldn´t be where I am today. On this note, I would like to address both of my parents: Mom, and especially Dad, thanks to all of your emotional and financial support, I was, and still am, able to pursue my biggest passion, which is the greatest gift I could ever wish for. I hope I can make you proud.

Table of Contents

Abstract 3

1. Introduction 4

2. Materials and Methods 8

2.1 Specimen Sampling 8

2.2 Light Microscopy 8

2.3 Scanning Electron Microscopy 8

2.4 Microcomputed Tomography 9

2.5 Histology – Serial Semithin Sectioning 9

2.6 Digitalization and Image Processing 10

2.7 Segmentation and 3D Reconstruction 10

2.8 Material Volumes 11

2.9 Length and Arrangement of the Intrinsic Galea Musculature 12

2.10 Biometric Measurements 12

3. Results 14

3.1 External Morphology 14

3.1.1 Proboscis 14

3.1.2 Sensilla Equipment 15

3.2 Internal Anatomy of the Feeding Apparatus 21

3.2.1 Proboscis Anatomy 21

3.2.2 Basal Galea Musculature and Stipes Pump 29

4. Discussion 34

4.1 Proboscis Morphology 34

4.1.1 Proboscis Length and Shape 34

4.1.2 Proboscis Tip 36

4.1.3 Sensilla and Cuticula 38

4.2 Proboscis Anatomy 41

4.2.1 Food Canal & Biomechanics of Honey Consumption 41

4.2.2 Internal Galea Musculature 43

4.2.3 External Galea Musculature 44

4.3 Advantages of Honey Feeding 45

Conclusion 46

References 47

Appendix 52

Zusammenfassung 52

Abstract

Varying proboscis morphologies in context with specialized feeding strategies are a reoccurring phenomenon in many lepidopteran lineages. Especially the death´s head hawkmoth, *Acherontia atropos* (Linnaeus, 1758), is a unique lepidopteran representative as it uses its ´ proboscis to penetrate sealed honeycombs and extract honey inside beehives rather than retrieve nectar from flowers. This distinct behavior has led to extensive research regarding various adaptations of *A. atropos*, such as chemical camouflage and proboscis anatomy in relation to sound production. Yet, recording detailed adaptations of the proboscis and stipes pump in light of food intake has been greatly neglected in the past. Therefore, in this study, morphological and anatomical analyses of the proboscis and stipes pump using serial semithin sectioning, microCT scanning as well as SEM imaging were conducted. Features of *A. atropos* were compared to *Agrius convolvuli* (Linnaeus, 1758), a long proboscid, nectar feeding relative. The findings highlight a unique morphology of the short, pointed proboscis in *A. atropos*. The food canal opening is elliptical and in a subterminal position - providing stability and even preventing possible blockages. Anatomically, both species share a principle external and internal galea muscle composition and an almost identical stipes muscle arrangement. Yet, internal galea muscle volume in *A. atropos* by far exceeds internal galea muscle volume in *A. convolvuli,* whereas stipes muscle volume does not. Basal galea muscle volume is only slightly larger in *A. atropos*. This clearly shows that some parts of the feeding apparatus, such as the proboscis, are highly specialized in *A. atropos,* while especially the ground plan of extra-galeal components appears to be more conserved among these related species.

1. Introduction

Lepidoptera comprise a large number of species, most of which are classified as Glossata. This taxon is most commonly associated with a proboscis that is used for fluid uptake (Krenn & Kristensen 2004; Mitter et al. 2017). In adults, the mandibles have been reduced whereas the maxillary components form the proboscis, built by the two galeae. The galeae are connected via dorsal and ventral legulae and thus enclose the food canal. Each galea contains internal galea musculature along with a trachea and a nerve (Krenn 1990). Typically, the internal galea muscles are involved in proboscis coiling, while the mechanism of uncoiling is based on a hydraulic system. Starting from its ´ resting position, the proboscis is elevated by the basal galea muscle. The subsequent contraction of the external stipes muscles causes an upward movement of the sclerotized part of the stipes and thus probably increases the pressure within the head cavity, pushing hemolymph into the galeae and causing the proboscis to uncoil (Krenn 1990; 2010). As parts of the stipes form a valve, the proboscis is stepwise uncoiled whenever the internal hemolymph pressure is increased. Recoiling is achieved by relaxation of the external stipes muscles, which in turn reopens the stipes valve. This assists the reflux of hemolymph back into the head cavity. The contraction of internal galea muscles, along with the elasticity of the cuticle, results in a coiling motion of the proboscis. With the contraction of the internal stipes muscle, the final resting position under the head is achieved (Wannenmacher & Wasserthal 2003; Krenn 2010). Yet, muscular equipment is not identical across all lepidopteran lineages. In Neolepidoptera, the basal galea muscle involved in proboscis elevation is normally comprised of two distinct muscle groups. They are both characterized by an origin which is located near the stipes-galea junction and run almost obliquely towards the dorsal galea wall. They are often almost perpendicular to one another as one runs more obliquely than the other. However, the level of distinguishability of these two muscles varies among different taxa (Krenn & Kristensen 2004). Intrinsic galeal muscles with an origin and attachment point located distal of the stipes and base region of the proboscis are considered an apomorphy of a more evolved lineage - the Ditrysia. The presence of at least some oblique galea muscles in Ditrysia is confirmed. Yet, multiple oblique lateral intrinsic muscles are seen as an apomorphy of the Apoditrysia. Distinct oblique lateral intrinsic and median intrinsic galea muscles are found within the Obtectomera and Macrolepidoptera (Krenn & Kristensen 2004). Given the high diversity of Macrolepidoptera – also regarding their feeding strategies – the similarities in the muscular groundplan of these butterflies indicates that lateral and median intrinsic muscles are involved in proboscis coiling regardless of the food source or feeding

technique. Different feeding strategies are therefore more likely to produce variations in tip morphology, sensilla density or proboscis length across different taxa. Although the lepidopteran proboscis is stated to have evolved only once (Krenn 2010), adaptations relating to different feeding guilds have been discussed by various authors (Krenn et al. 2001; Kitching 2003; Petr & Stewart 2004; Zaspel et al. 2011; Zenker et al. 2011; Plotkin & Goddard 2013; Lehnert et al. 2016).

Previous studies have divided the proboscis of butterflies into distinct functional regions (Eastham & Eassa 1955; Krenn 1990). Here, the proximal and distal region are typically separated by a knee bend at approximately one third of the proboscis length (Eastham & Eassa 1955; Krenn & Mühlberger 2002). This bend region can typically be observed when the proboscis is uncoiled while feeding. Here, the proximal region of the proboscis is extended horizontally while the knee bend arches downward. From the bend region on, the distal proboscis extends more vertically (Krenn 1990). Accordingly, the proximal region is located at about 30% of the entire proboscis length while the distal region is defined as being at 60% of the proboscis length. The tip region, which facilitates fluid uptake, is located at 90% of the proboscis length.

Flower visiting lepidopterans, which typically feed on nectar, possess longer proboscises relative to their own body length (Lehnert et al. 2016). The tip is characterized by prominent drinking slits formed by dorsal legulae (Krenn 2010). Non-flower visiting species on the other hand, often exhibit modifications of the proboscis tip. Here, sensilla styloconica, sensory organs responsible for chemo- and mechanoreception (Ma et al. 2019), can exhibit a brush-like arrangement at the apex of the proboscis. As sensilla styloconica are hydrophilic, they act as a nano-sponge when placed on a wet surface, collecting fluid for the butterfly to ingest (Lehnert et al. 2016). Such species will often feed on tree sap, extrafloral nectars, sugary exudates of plant-feeding insects or juice leaking out of decaying fruit (Krenn et al. 2001; Ma et al. 2019). Sphingids, which are placed within the Macrolepidoptera, display great interspecific differences in proboscis length. The proboscis may be extremely long in some species while being very short or even reduced in others (Powell 2009; Smola 2021). Most sphingids, such as the convolvulus hawk-moth, *Agrius convolvuli* (Linnaeus, 1758), are nectar feeders and therefore play an important role in flower pollination (Powell 2009). For many hawkmoths, the presence of a knee bend is clearly noticeable in feeding individuals (Fig 1). Some groups lack sensilla styloconica entirely, which is speculated to be an adaptation to the emersion of the proboscis while feeding (Petr & Stewart 2004).

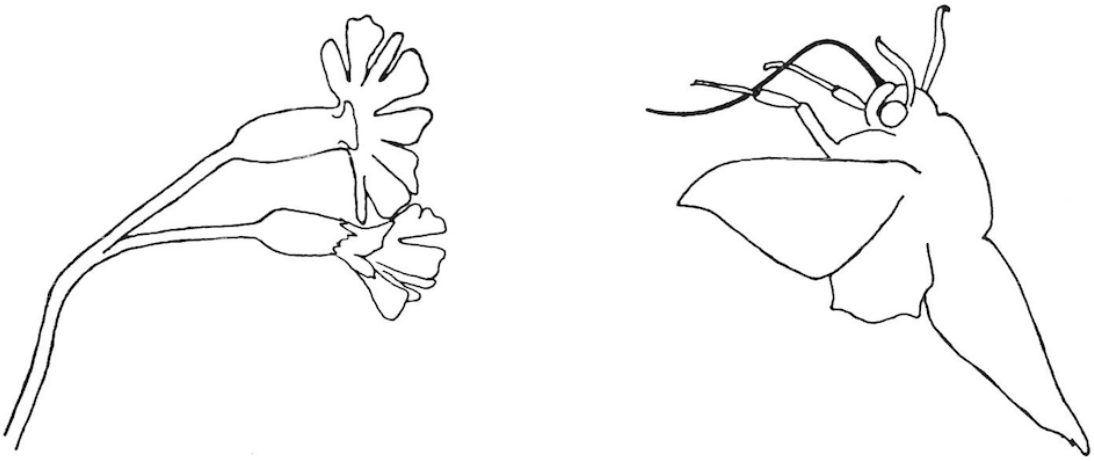

Fig 1. *Deilephila elpenor* (Linnaeus, 1758) (Sphingidae) flying to a flower. A clear bend of the proboscis is visible. Image from Bänziger 1971.

However, some Sphingidae have developed different feeding strategies. As a non-flower visiting species, the death´s head hawkmoth *Acherontia atropos* (Linnaeus, 1758) exhibits a very unusual feeding habit. All three species of the genus *Acherontia* are speculated to ingest honey rather than nectar (Kitching 2003). So far, this has only been confirmed for *A. atropos* (Moritz et al. 1991; Kitching 2003). Adult individuals are known to invade beehives of *Apis mellifera* (Linnaeus, 1758) in order to feed on honey. The short, robust and sharply pointed proboscis of this species is therefore interpreted as an adaptation for penetrating sealed honeycombs (Kitching 2003). In order to reach the honeycombs, *A. atropos* must first successfully infiltrate bee colonies without being attacked and subsequently killed. Therefore, the moth´s body surface emits a specific array of saturated and unsaturated fatty acids. This chemical composition is also found on worker bees, making *A. atropos* olfactorily indistinguishable from members of the colony and thus camouflaging the moths inside the beehive (Moritz et al. 1991). Another unusual feature of this species is its´ ability to produce sound by inhaling and exhaling air through the proboscis (Brehm et al. 2015). This has led to a multitude of studies analyzing the moth´s mouthparts in conjunction with sound production. As for *A. atropos*, its´ distinct lifestyle has made it subject to various investigations. Although this species is well studied, detailed adaptations of the feeding apparatus regarding honey intake remain unclear. Therefore, the aim of this study is to examine which morphological and anatomical adaptations of the feeding apparatus have evolved to enable the unique feeding habits of this species. To do so, histological sectioning, 3D reconstruction, SEM imaging and

biometric measurements of the proboscis as well as 3D analyses of the stipes pump were performed. For comparison, data for the nectar feeder *A. convolvuli*, a relative of *A. atropos,* was obtained. Assumably, the ground plan of the proboscis and the stipes pump are similar in both species. Yet, differences in proboscis morphology, sensilla distribution and muscular distribution are expected. Due to a robust and broad proboscis, galea muscle- and galea volume in *A. atropos* are predicted to be larger than in *A. convolvuli*. Furthermore, a larger feeding canal is theorized to enable honey consumption in this species. Even though the proboscis of *A. atropos* is anticipated to be highly specialized, a similar ground plan of the stipes pump in both compared species is expected.

2. Materials and Methods

2.1 Specimen Sampling

Several *A. atropos* specimens were provided by Manuel Staggl, BSc. The moths were delivered to the lab in the Integrative Zoology (University of Vienna) as pupae and adult individuals were euthanized with carbon dioxide after hatching. Specimen Le520R was then selected for histological sectioning and microcomputed tomography. Different individuals were selected for scanning electron microscopy and conducting biometric measurements (Le520). The *A. convolvuli* specimen S35 selected for histological sectioning and microCT scanning was sampled in the 16th district in Vienna using a net. It was then fixed in a mixture of formalin, ethanol and acetic acid (FAA). The *A. convolvuli* specimen Le21 used for biometric measurements as well as additional proboscises of both species for SEM and light microscopy were taken from the insect collection of the Department of Evolutionary Biology, where they had been stored in 70% ethanol (EtOH).

2.2 Light Microscopy

Light microscopy was applied for counting proboscis coils and analyzing sensilla equipment (Table 2). Dried, pinned specimens of *A. atropos* and *A. convolvuli* from the insect collection were used. The proboscises were removed with small scissors and kept in 30 % lactic acid for several days before glycerin embedment. They were viewed with a Nikon eclipse E800 microscope (Nikon, Tokyo, Japan).

2.3 Scanning Electron Microscopy

Upon preparation for SEM imaging, the proboscis of an *A. atropos* specimen was removed mechanically from an individual which previously had been fixed in FAA and stored in 80% EtOH. The FAA was prepared by mixing 50ml concentrated formalin (=35%), 150 ml 80% EtOH and 15 ml concentrated acetic acid, which yielded 215 ml in total. A separate, severed head as well as a proboscis tip were also used. For *A. convolvuli*, the tip and proximal region were separated from a proboscis which had been stored in 80% EtOH. All samples were dehydrated with an ascending EtOH series (1x 96%, 3x 100%, 30 mins/step), submerged in hexamethyldisilazane and air dried overnight (Bock, 1987). They were then mounted on stubs fitted with graphite plates and coated with gold. SEM imaging was performed on a Philips

XL30 ESEM (Philips, Amsterdam, Netherlands) at 15 kV. All Images were viewed and saved with Scandium (Olympus, Tokio, Japan).

2.4 Microcomputed Tomography

Specimens of *A. atropos* and *A. convolvuli* were fixed in FAA and stained with 1% iodine in EtOH. MicroCT scans of both species were performed with an Xradia MicroXCT (Carl Zeiss X-Ray Microscopy, Jena, Germany) imaging system. For *A. atropos*, scans were conducted at an optical magnification of 1. The specimen was scanned at 60kV peak source and 133 μA intensity. Images were taken in the tomography imaging mode. Projections were acquired with a 20 sec exposure time (camera binning=1). The resulting slices were 1280 x 1280 pixels in size and images yielded a pixel resolution of 7.2894 x 7.2894 μm (7.2894 x 7.2894 x 7.2894 voxel size). For *A. convolvuli*, scans were performed at 80 kV peak voltage and 100 μA intensity at an optical magnification of 0.4. Images were taken with an exposure time of 15 sec and yielded a pixel resolution of 5.038 x 5.038 μm (5.038 x 5.038 x 5.038 voxel size). Tomographic reconstructions were made with the XMReconstructor software supplied with the system and volume renderings of the scans were performed in Amira 6.4.0 (Visage Imaging, Richmond, Australia).

2.5 Histology – Serial Semithin Sectioning

The proboscises of both species were removed from the head after being fixed in FAA. The proboscises were kept in FAA for two days and then stored in 70% EtOH until dehydrated with an ascending EtOH series (3x 70%, 1x 80%, 1x 90%, 1x 96%, 3x 100%). Each dehydration step was applied for 10 mins. This was followed by an acetone wash, which was repeated twice. Each washing step was applied for 10 mins. The proboscises were kept in a 50 : 50 resin-acetone mixture overnight, transferred to a 80 : 20 mixture for six hours and then kept in pure resin overnight before being fitted into a mold. Polymerization was induced at 60°C.

1 μm semi-thin sections were cut using a Leica UC6 ultracut microtome (Leica, Wetzlar, Germany). At least 200 μm of serial cross sections were acquired for the proximal, distal and tip region of the proboscises of *A. atropos* and *A. convolvuli*. The series were transferred onto microscope slides and stained with toluidine blue for 20 seconds. Lastly, the slides were sealed with acrylic low viscosity resin and covered with cover slips.

2.6 Digitalization and Image Processing

For both species, 200 µm of every proboscis region (proximal, distal and tip) were photographed, which yielded six image stacks. Thereby, the proximal region was appointed to 30%, the distal region to 60% and the tip region to 90% of the entire proboscis length. For *A. atropos* respectively, additional 1367 µm of the proboscis tip were digitalized for later 3D reconstruction. All sections of the proboscises were photographed with a Nikon eclipse E800. Different proboscis sections of the two species were photographed by applying different magnifications and exposure times (Table 1). To calculate voxel size, photos of a micrometer scale were taken while operating under the same individual magnifications as the stacks of the different regions. Using the scale as a reference in Photoshop, a length of 1000 µm or 500 µm was defined with the rectangle tool. For every region, this determined the amount of pixels equivalent to this length. The results were then downscaled to one pixel to determine voxel size (Table 1).

Images of faulty sections were deleted and replaced by either the sections before or after. The image stacks were then converted from RGB to BW and image size was reduced by 50% in Photoshop CC 2018 (Adobe Systems, San Jose, USA). For images of the micrometer scale, the same procedure was applied before taking any measurements.

Table 1. Magnifications / exposure times applied for photographing histological sections of the tip, distal and proximal proboscis regions in *A. atropos* and *A. convolvuli* as well as the calculated voxel sizes. Proximal region at 30% of the proboscis length, distal region at 60% of the proboscis length and tip region at 90% of the proboscis length

	Proboscis region		
	proximal	**distal**	**tip**
A. atropos	4x -1.25 / 1ms	4x -1.25 / 1ms	10x / 1ms
Voxel size	1.179 x 1.179 x 1	1.179 x 1.179 x 1	0.59 x 0.59 x 1
A. convolvuli	10x / 1ms	10x -1.25 / 4ms	10x -1.5 / 4ms
Voxel size	0.592 x 0.592 x 1	0.469 x 0.469 x 1	0.392 x 0.392 x1

2.7 Segmentation and 3D Reconstruction

All image stacks were aligned in Amira 6.4.0 using the automatic alignment tool, incorrectly aligned pairs were arranged manually. For each of the six 200 µm stacks, a volume rendering (volren tool) and a scalebar (scalebar tool) were generated to check for any distortions or wrong

size ratios resulting from a potentially incorrect voxel size. Lateral intrinsic muscles, median intrinsic muscles, the galeae and the food canal were segmented in the segmentation window using the threshold, the brush tool and the interpolation tool. The selections were then added to individual materials and saved in a labels file for every stack.

Separately, lateral and median intrinsic muscles were also segmented in the 1367 µm stack of the proboscis tip of *A. atropos*. For visualization of the tip itself, a volume rendering was generated with the volren tool and a grey colourmap. The segmented musculature was displayed by generating an Iso-surface of the created materials, reducing the number of faces, smoothing the surface and enabling the surface view. Snapshots were saved as TIFF files, the values for render tiles and antialias were increased to 3 to improve image quality.

The same procedure was applied to the segmentation and visualization of the basal galea musclulature, the internal stipes muscles, the external stipes muscles and the head capsule from the microCT scans of one *A. atropos* and one *A. convolvuli* specimen.

2.8 Material Volumes

For each of the six 200 µm stacks, the volume of the lateral intrinsic musculature, median intrinsic musculature, the galeae and the food canal was computed based on the materials created in Amira. In this case, the volume of the lateral and median intrinsic musculature was calculated for each galea separately. For the galeae, volume computation was performed including the intrinsic musculature. Based on the labels file, the individual volumes were computed and displayed by applying the material statistics tool and selecting the materials as source. The same principles were applied for volume computation of the basal galea muscle, external stipes muscles (esm), internal stipes muscle (ism) and head capsule based on the microCT scans of both species. For the stipes musculature (esm, ism) and basal galea musculature, combined values of the left and right side are presented, as individual volumes of the left and right side were always identical. All results were recorded in Excel 16.48 (Microsoft, Redmond, USA). The volume unit was thereby defined by the voxel size. All values were transformed to mm^3. For all volumetric percentages and size ratios, data from the left and right galea or side was combined.

For projection of muscle volume onto the entire proboscis length of *A. atropos* and *A. convolvuli*, lateral and median intrinsic muscle volume was combined for each proboscis region. Muscle volumes of the proximal, distal and tip region were each extrapolated to a third

of the proboscis length. To estimate the total muscle volume, the values of each region were added up.

2.9 Length and Arrangement of the Intrinsic Galea Musculature

Designated muscle fibers were selected for analyzing length and arrangement of the lateral intrinsic galea musculature for the different species and proboscis regions in Amira. Therefore, only fibers including an observable proximal origin as well as a distal insertion point were chosen. In *A. atropos*, 1 lateral muscle fiber from the tip, distal and proximal region was measured. For *A. convolvuli*, 2 lateral fibers from the tip region (1 from the left galea, 1 from the right galea), 1 lateral fiber from the distal region (left galea) and 5 lateral muscle fibers from the proximal region (2 from the left galea, 3 from the right galea) were selected. Due to their length and arrangement, median muscles could not be measured. The length of the fibers was determined in the segmentation window by counting the number of slides between the origin and insertion point. Due to a section thickness of 1 µm, one slide approximated to 1 µm. Muscular angles of slope were determined using surface generations and the arithmetic tool in Amira. Measurements were taken from the dorsal connection to the galea wall to the proximal point of origin. A line drawn along the longitudinal galea axis acted as a reference. In *A. atropos*, only the muscle fiber from the tip region was measured using this technique. Muscle fibers from the distal and proximal region were measured using the microCT scan of the same *A. atropos* specimen. Thereby, muscle fiber length and muscular angles of slope were determined using ortho slices and the arithmetic tool in Amira. Muscle angles were determined by applying the same principle as in the other proboscis regions. All presented angle values for both species and muscle fiber lengths of the distal and proximal region in *A. atropos* are approximations.

2.10 Biometric Measurements

The width of the head capsules was measured on specimens fixed in FAA and stored in 80 % EtOH using a caliper. For further reference, head capsule width was also evaluated using the arithmetic tool on the microCT scanned specimens in Amira. Measurements were always taken from the outer most edge of one eye to the other.

Proboscis lengths were determined based on the microCT scans of *A. atropos* and *A. convolvuli*. Measurements were taken from the dorsal side of the galeae using the arithmetic tool in Amira.

Therefore, multiple 2D lines were drawn along the longitudinal axis of the proboscis. The sum of all line values amounted to the proboscis length.

Individual sensilla lengths were determined in Photoshop by applying the rectangle and ruler tool. Therefore, SEM images of one *A. atropos* and one *A. convolvuli* specimen were used as a reference. For sensilla stylus and bristle length, measurements were taken from the base to the apex of the sensillum. Apical sensory cones were included for estimating sensilla styloconica length. Bristle size of sensilla trichodea varied within the same proboscis region in *A. atropos*. Thus, approximately 3-5 sensilla were measured. For bristle shaped sensilla of the proximal region, shortest and longest sensilla lengths were documented. In *A. covolvuli*, sensilla trichodea of the proximal galea region and internal sensilla basiconica were not visible in SEM images and were too small to be accurately counted or measured under the light microscope. However, proper identification was still possible.

The same Photoshop tools were applied for measuring cuticula thickness and food canal diameter (Table 2). Measurements were taken from histological sections the proximal region as both parameters did not notably change throughout the proboscis. Food canal diameter was determined at the widest part of the canal. Cuticula width was measured at the thickest region on the dorsal side of the galea.

Table 2. Overview of methods applied for analyzing different traits in *A. atropos* and *A. convolvuli*.

Trait	**Method**
Proboscis morphology	SEM
Sensilla distribution	Light microscopy
Sensilla morphology	SEM
Sensilla length	SEM, Photoshop
Proboscis length	MicroCT, Amira
Head capsule diameter	Fixed specimen, caliper
Galea anatomy	Semithin sections, Amira
Cuticula width, Food canal width, Proboscis diameter	Semithin sections, Photoshop
Internal galea muscle-, Food canal- and Galea volume	Semithin sections, Amira
External galea muscle anatomy	MicroCT, Amira
External galea muscle volume	Micro CT, Amira

3. Results

3.1 External Morphology

3.1.1 Proboscis

Although *A. atropos* and *A. convolvuli* both share a basic proboscis composition, they exhibit distinct differences in proboscis morphology. In *A. atropos*, the proboscis measures a total length of 12.4 mm and is wound up in ¾ of a coil in resting position (Fig 2a). The proboscis tip tapers at the apex and is therefore sharply pointed. Within the tip region, the galeae form a large, elliptical opening of the food canal, located subterminally of the apex (Fig 3b). Throughout the rest of the proboscis, the food canal is enclosed by the galeae which are connected by dorsal and ventral legulae. Ventral legulae extend from the proboscis base to the apex while dorsal legulae are absent in the tip region (Fig 2c, 3b, 6a). Ventral legulae are similar in structure across all proboscis regions. The linkages are arranged in double hooks and act as a stable junction between the two galeae (Fig 3b). Dorsal legulae are plate shaped and overlap with the legulae of the opposite galea. They are arranged in a single row while partially covering one another. The external wall of the galeae is composed of regular, vertical cuticular ribs. These ribs curve slightly towards the apex. They extend into the ventral and dorsal linkages and exert a bend towards the apex within the dorsal region. Also, short ridges alternate between dorsal and ventral parts of the ribs in the dorsal region of the galeae. The ribs do not fully extend into the tip region and fade into the ventral side of the tip. Therefore, the cuticula surrounding the food canal opening is smooth (Fig 2b, 3b). At the proboscis base, the dorsal galea wall displays short, densely packed microtrichia (Fig 3a). In this case, they are hair-like in appearance and form a contact point for the pilifers. The food canal is lined with smooth, uniform cuticular ribs, arranged vertically throughout the entire proboscis. Similarly to external cuticular ribs, they extend into the ventral and dorsal linkages.

In *A. convolvuli*, the proboscis is wound up in 6.5 coils in resting position (Fig 2d) and measures approximately 70.5 mm in length. The proboscis tip is blunt ended. Dorsal and ventral legulae enclose the food canal throughout the entire proboscis. Therefore, ventral and dorsal legulae are present from the base region to the apex. Ventral legulae are arranged as double hooks and are tightly packed along the longitudinal axis. Dorsal legulae are plate shaped and feature tipped upper branches (Fig 2f). They overlap with linkages of the opposing galea. Within the tip region, prominent dorsal legulae are loosely arranged to form drinking slits for nectar

consumption. Furthermore, they close the proboscis tip at the apex (Fig. 2e, f). At the proboscis base, the dorsal wall of the galeae is covered by short microtrichia. The galeae are characterized by external cuticular ribs which are curved towards the apex of the proboscis. The ribs are present throughout the entire proboscis. They also extend up to the ventral and dorsal legulae. Within the lateral galea region, short ridges occur between the ribs. Furthermore, the cuticular ribs display a ventro-lateral bend towards the proboscis base (Fig 4f). The wall of the food canal is covered in narrow, vertical cuticular ribs interspaced by short ridges.

3.1.2 Sensilla Equipment

In *A. atropos* and *A. convolvuli*, the exterior wall of the galea displays four morphological sensilla types: Sensilla trichodea, external sensilla basiconica, sensilla styloconica and long bristle shaped sensilla. Only one type of interior sensilla basiconica line the wall of the food canal (Table 3). All morphological sensilla types show the same structural composition in both species.

In *A. atropos*, s. trichodea are arranged in 3 rows, placed along the ventral, ventro-lateral and dorsal galea region. Ventral s. trichodea extend from the proximal proboscis region to the apex of the apical drinking region. At the base of the proboscis, they are replaced by long bristle shaped sensilla (Table 3). Ventro-lateral s. trichodea are present from the distal to the tip region of the proboscis. In the tip and distal region, about 16 s. trichodea are distributed loosely along the longitudinal galea axis. Dorsal s. trichodea are only found within the tip region. They exhibit an irregular arrangement and are often paired with s. styloconica. Ventral and dorsal s. trichodea demonstrate the highest densities in the tip region of the proboscis. In *A. convolvuli*, s. trichodea are distributed loosely in a lateral and ventral line within the tip region. Throughout the distal region of the proboscis, only few, irregularly placed sensilla are found within the dorsal, lateral and ventral area of the galeae. Within the outermost coil, s. trichodea exhibit slightly higher densities. They are replaced by long bristle shaped sensilla at the proboscis base (Table 3). Sensilla trichodea are characterized by a bristle extending from a circular, cuticular indentation (Fig 4a, d). In *A. atropos*, the bristle may vary in length, even within the same galea region. Within the tip region, s. trichodea length therefore ranges from 11.5 – 33.3 µm. Sensilla trichodea of the proximal galea region are approximately 31.2 – 43 µm long (Table 3). In the tip region of *A. convolvuli*, the bristle is typically 20.4 µm long but may also vary in length depending on the proboscis region (Table 3).

Sensilla basiconica of the exterior surface protrude from a circular, cuticular depression and consist of a blunt-tipped sensory cone with an apical pore (Fig 4a, d). Sensory cones of the tip region are of similar length in both species, measuring 6.5 µm in *A. atropos* and 5 µm in *A. convolvuli* (Table 3). In *A. atropos*, s. basiconica are present within the dorsal and dorsolateral tip region as well as the distal proboscis region. They extend into the apex of the proboscis. In the apical drinking region of *A. convolvuli*, s. basiconica extend longitudinally along the border between dorsal legulae and the galea. Only few s. basiconica are present within the proximal galea region. Here, they measure approximately 3 – 4.2 µm in length (Table 3). In both species, internal s. basiconica of the food canal are arranged in a dorsal line from the base of the galea to the apical drinking region. The sensilla are spaced more loosely in the distal proboscis region and exhibit higher densities at the base and tip. In *A. atropos*, approximately 21 s. basiconica line the food canal. Their cones are bristle-like in appearance and protrude approximately 26 – 27.6 µm from a somewhat elevated cuticular surface (Table 3).

Within the tip region of *A. atropos*, s. styloconica are arranged in two rows extending into the apex (Fig. 2b). The dorsal row enclosing the food canal opening thereby consists of about 5 – 6 s. styloconica per galea (Fig 3b). The second row extending from the apex into the distal proboscis region shows an arrangement of approximately 24 sensilla on one galea. The space between the individual sensilla slightly increases in proximal direction of the galea. Sensilla styloconica are only found in the tip and distal proboscis region. In *A. convolvuli*, s. styloconica exhibit substantially lower densities than in *A. atropos*. The proboscis tip therefore only displays 4 – 5 s. styloconica (Fig 2e). In the lateral tip region, they are typically followed by a s. basiconicum, a s. trichodeum and another s. basiconicum. Within the ventral tip region, each s. styloconicum is followed by a s. trichodeum. Sensilla styloconica are only present in the tip / distal region of the galea (Table 3). In both species, cylindriform aspinate (Petr and Stewart 2004) s. styloconica extend from a groove-like depression of the cuticle. They are composed of a stylus and a pointed sensory cone protruding from the tip (Fig 4b, e). The stylus is characterized by a smooth shaft. Only in *A. convolvuli*, the shaft tapers towards the base and forms a slender stem (Fig 4e). The tip of the stylus is typically dome shaped. Sensilla styloconica are larger in *A. atropos*, measuring approximately 35.5 µm in length. In *A. convolvuli* sensilla are typically 24.8 µm long (Table 3).

At the proximal galea region, the cuticular wall is covered in long hair-like sensilla (Fig 4c, f). The bristles extend from a minor cuticular depression and are tilted slightly towards the apex

of the proboscis. In *A. atropos*, one galea encompasses > 150 long bristle shaped sensilla. In *A. convolvuli*, only about 35 bristle shaped sensilla are found in approximately the same galea area. Bristle length ranges from approximately 105 – 646 µm in *A. atropos*. The longest sensilla in *A. convolvuli* are shorter than the longest sensilla in *A. atropos*, exhibiting lengths of up to 586 µm (Table 3). In both species, the longest bristle shaped sensilla are located on the ventral side of the galea (Fig 4c, f).

Table 3. Length and distribution of sensilla types in the short proboscid *A. atropos* (n=1) and the long proboscid *A. convolvuli* (n=1) according to proboscis region (proximal, distal, tip). For each sensilla type 1 - 5 individual sensilla were measured. st - sensilla trichodea, sb1 – external sensilla basiconica, sb2 – interior sensilla basiconica, ss – sensilla styloconica, bs – bristle shaped sensilla. "x" - sensilla present. " / " - unable to measure sensilla length.

	A. atropos				*A. convolvuli*			
External sensilla	**st**	**sb1**	**ss**	**bs**	**st**	**sb1**	**ss**	**bs**
Proximal	x			x	x	x		x
length (µm)	31.2 - 43			105 - 646	/	3 - 4.2		< 586
Distal	x	x	x		x		x	
Tip	x	x	x		x	x	x	
length (µm)	11.5 - 33.3	6.5	35.5		20.4	5	24.8	
Internal sensilla		**sb2**				**sb2**		
Food canal wall		x				x		
length (µm)		26 - 27.6				/		

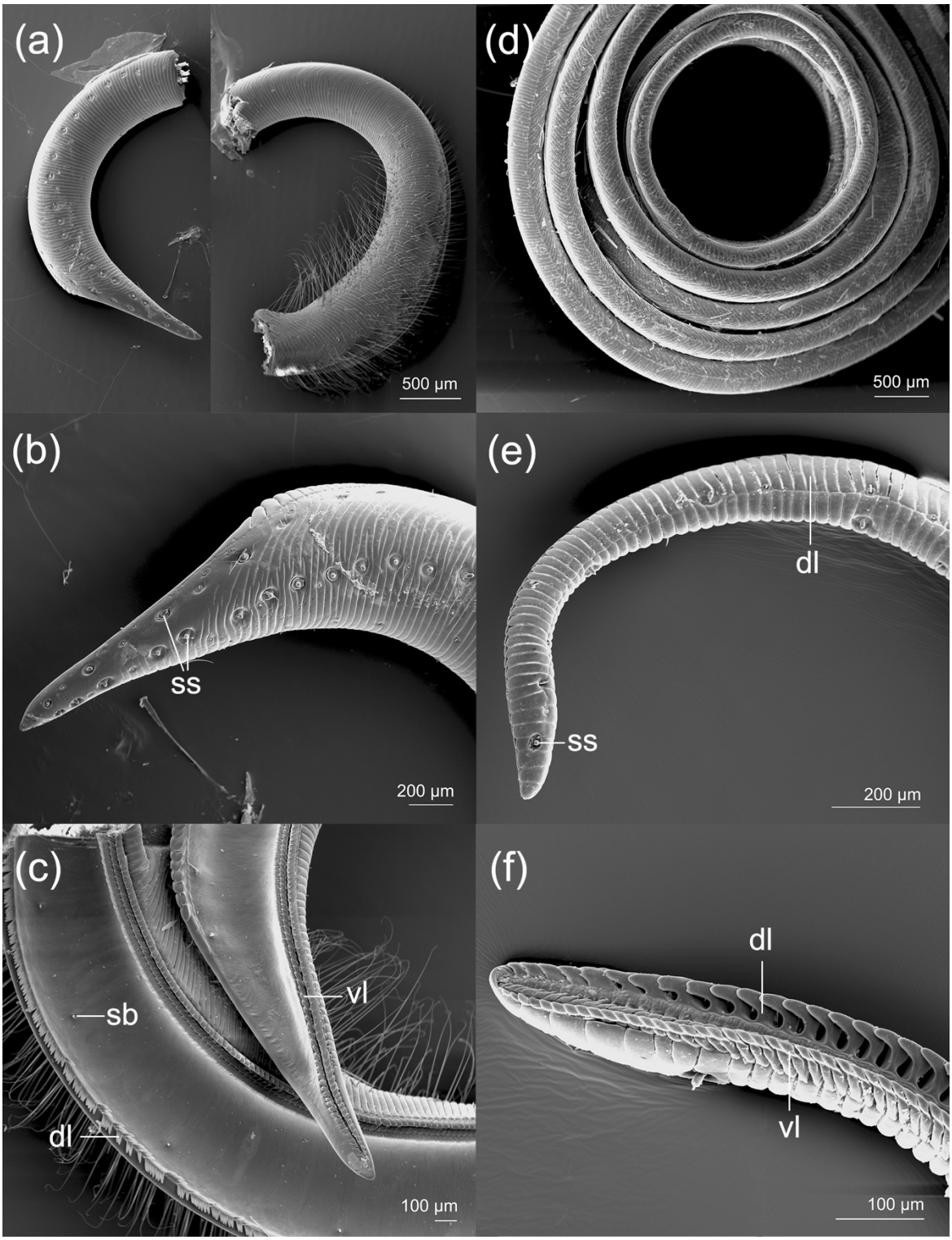

Fig. 2. Proboscises of *A. atropos* **(a-c)** and *A. convolvuli* **(d-f)** (SEM). **(a)** Left galea. Lateral view. The proboscis forms ¾ of a coil in resting position. The galea is coiled more strongly due to chemical dehydration. For imaging purposes, the galea was separated into two parts. **(b)** Proboscis tip. Sensilla styloconica (ss) are arranged in a dorsal and a lateral row. The galea wall surrounding the food canal is smooth whereas the rest of the galea is covered with cuticular ribs. **(c)** Inner galea wall of the tip and base region. Dorsal legulae (dl) are absent in the tip region while ventral legulae (vl) reach the apex. The food canal is lined with internal sensilla basiconica (sb) **(d)** Proboscis overview. Lateral view. The long proboscis is wound up in 6.5 coils in resting position. **(e)** Tip region. Lateral view of the left galea. Dorsal legulae close the apex of the tip. Few sensilla are present. **(f)** Inner galea wall. Median view. Prominent dorsal legulae form drinking slits and close the tip at the apex.

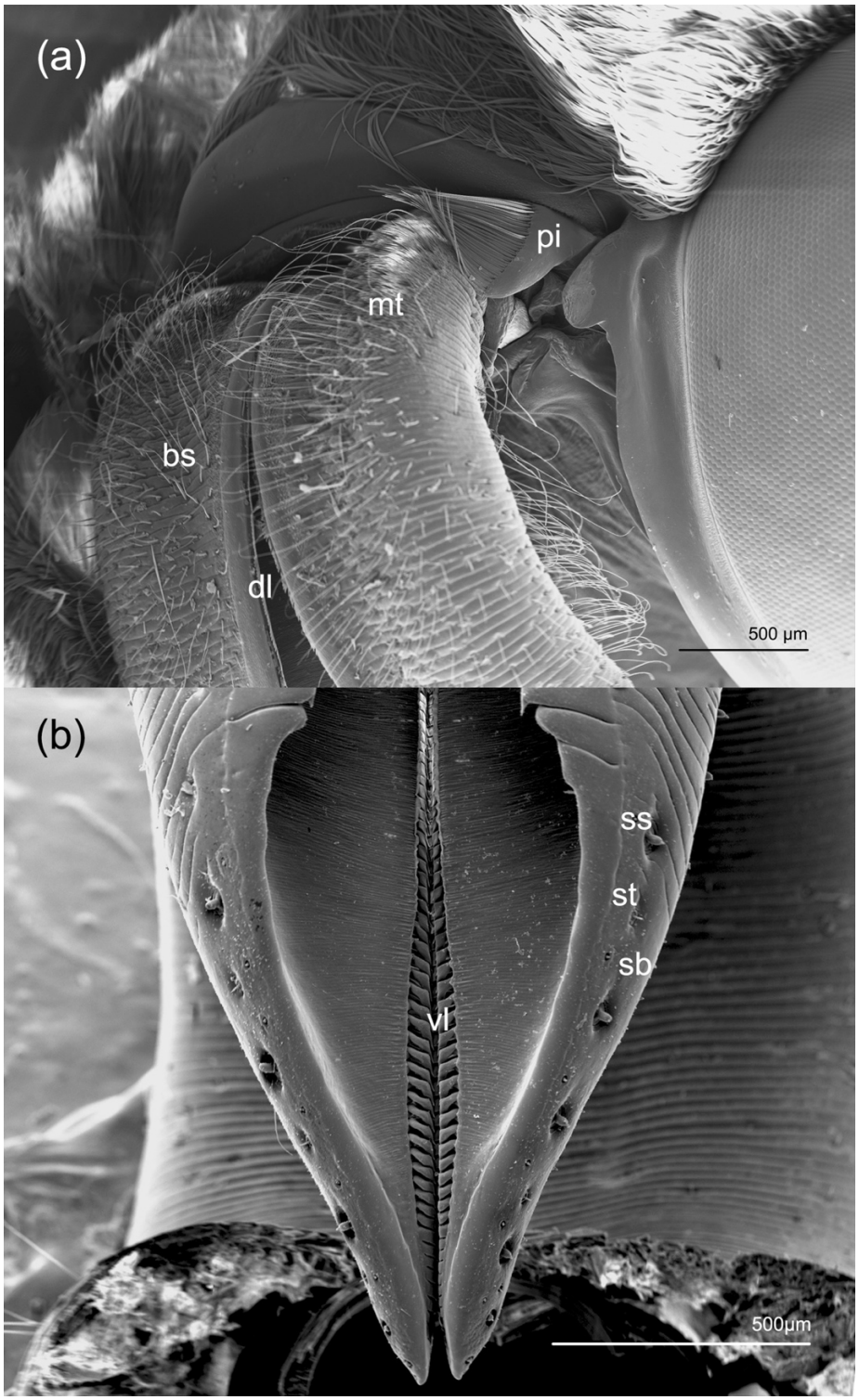

Fig 3. Proboscis of *A. atropos* (SEM). **(a)** Proximal proboscis region and head capsule. The dorsal side of the proboscis base is covered by short microtrichia (mt) and long bristle shaped sensilla (bs). Dorsal microtrichia function as a contact point for the pilifers (pi). Dorsal legulae (dl) overlap with dorsal linkages of the opposite galea, the gap between the galeae is an artefact caused by chemical dehydration. **(b)** Dorsal view of the proboscis tip. The elliptical opening of the food canal is positioned subterminally of the apex. Sensilla styloconica (ss), sensilla trichodea (st) and sensilla basiconica (sb) surround the food canal opening. Dorsal legulae are absent in the immediate tip region whereas ventral legulae (vl) reach the apex of the galeae.

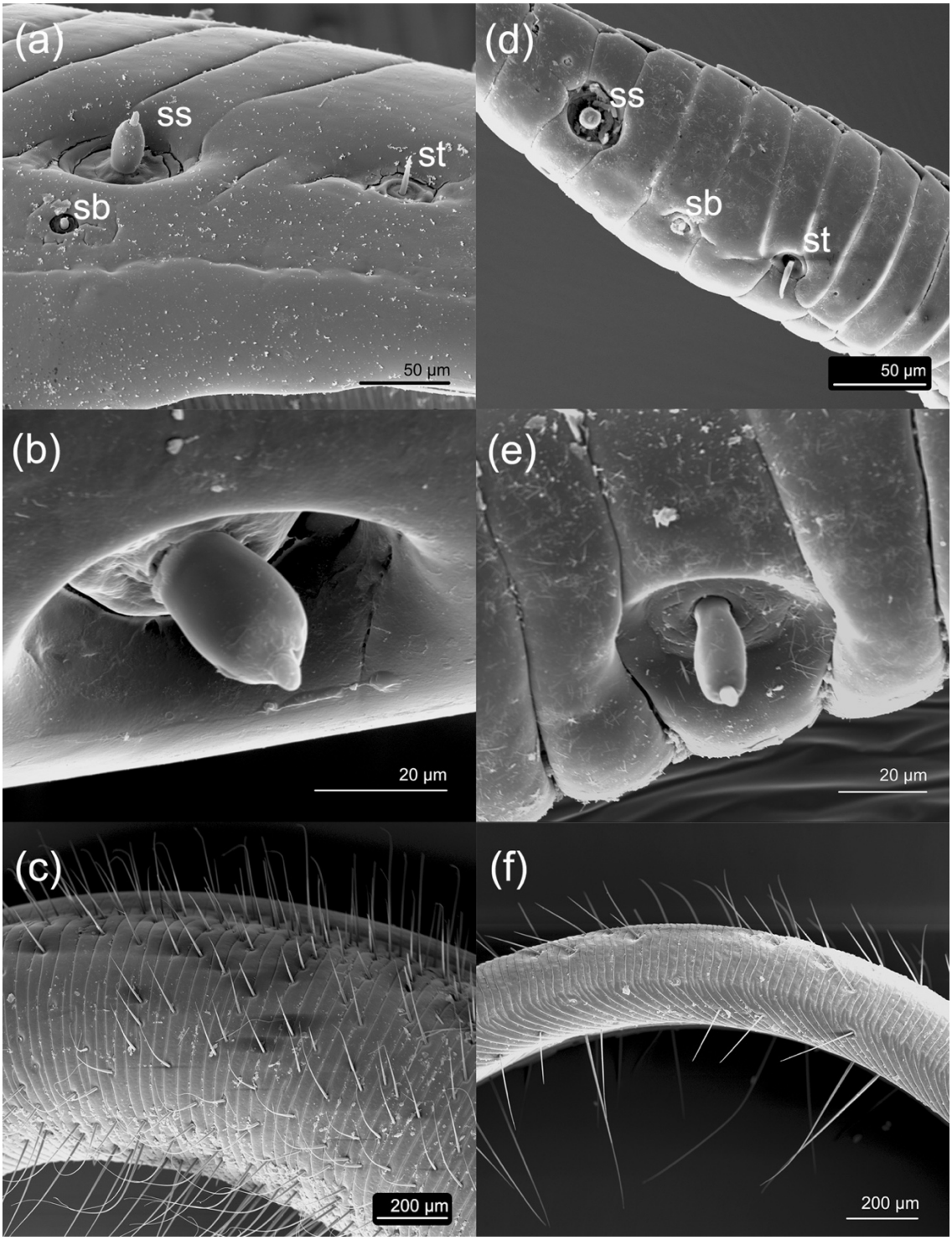

Fig 4. Sensilla equipment of *A. atropos* **(a-c)** and *A. convolvuli* **(d-f)** (SEM). **(a)** Cuticular wall of the tip region displaying 3 morphological sensilla types: Sensilla styloconica (ss), sensilla basiconica (sb) and sensilla trichodea (st). **(b)** Cylindriform aspinate sensillum styloconicum from the tip region. The sensillum is composed of a stylus and a sensory cone. **(c)** Bristle shaped sensilla from the proximal proboscis region. The longest sensilla are located on the ventral side of the galea. All sensilla are tipped towards the apex of the proboscis. **(d)** Proboscis tip of *A. convolvuli* showing sensilla styloconica, basiconica and trichodea. **(e)** Cylindriform aspinate sensillum styloconicum from the tip region. The stylus of the sensillum forms a slim shaft at the base. **(f)** Bristle shaped sensilla of the proximal proboscis region. Sensilla are loosely arranged. The longest sensilla are located on the ventral side of the galea.

3.2 Internal Anatomy of the Feeding Apparatus

3.2.1 Proboscis Anatomy

In *A. atropos*, the diameter of the galeae displays a substantial decrease from the proximal to the tip region while the diameter of the food canal stays more or less constant (Fig 5a-c, Table 5). Therefore, the proboscis diameter decreases from 1950 µm in the proximal region to 1437 µm in the distal region and 910 µm in the tip region (Table 5). The galeae are sickle-shaped in cross section at the tip while adopting a rounder shape towards the proboscis base. The cuticula encompassing the galeae is approximately 80.3 µm thick (Table 5). Each galea contains one trachea, one nerve and musculature. Tracheae and nerve cords extend longitudinally from the base of the proboscis to the apex, while internal galea muscles reach into the tip region, but do not fully extend into the apex (Fig 6b-d). Overall muscle volume decreases from the proximal proboscis region to the tip. Yet, within the distal region, the internal galea musculature makes up the largest percentage of the galea volume (Table 6). Lateral intrinsic muscles as well as median intrinsic muscles are present throughout the tip, distal and proximal region. Both, lateral and median intrinsic muscles, are arranged in multiple muscle strands and are separated by a tendon. The lateral intrinsic musculature is typically composed of 8-18 individual fibers in one cross-section, depending on the proboscis region (Fig 5). It is characterized by a lateral origin as well as a dorsolateral progression (Fig 5, 7). In the tip region, a muscle fiber extends at an approximate angle of 18.1° and has a length of 572 µm. A lateral muscle fiber from the distal galea region, measures approximately 670 µm in length and extends at an angle of 22.3°. In the proximal galea region, a lateral muscle fiber measures 768 µm in length and extends at an approximate angle of 35° (Table 4). Lateral muscle fibers from the proximal proboscis region may therefore be longer and extend at a steeper angle of slope than muscle fibers from the distal and tip region. The median intrinsic musculature originates in the ventro-lateral region of the galea and extends longitudinally along the ventral axis (Fig. 7). It typically encompasses 7-9 individual fibers per cross-section (Fig. 5). In all proboscis regions, lateral intrinsic muscle volume exceeds median intrinsic muscle volume and makes up a higher percentage of the galea volume (Table 6). Therefore, lateral intrinsic muscles are more strongly developed throughout the entire proboscis than median intrinsic muscles. In the tip region, distribution and relative amount of lateral and median intrinsic muscles differs between the two galeae and is therefore not symmetrical in the studied specimen (Fig 7). Here, lateral intrinsic muscle volume of the left galea is more than twice as large as lateral muscle volume of the right galea (Table 6).

In *A. convolvuli*, the galeae decrease in size from the proximal region to the tip while the diameter of the food canal stays more or less constant (Fig 5, Table 5). Therefore, the proboscis diameter is 827.5 µm in the proximal region, 771 µm in the distal region and 533.3 µm in the tip region (Table 5). The proximal galeae are rather wide in cross-section and acquire a half-moon shape towards the proboscis tip. Cuticula thickness is approximately 59.2 µm (Table 5). Tracheae, nerve cords as well as the intrinsic galea muscles extend throughout the entire proboscis. Nerve cords are substantially larger in proximal and distal regions and even exceed the relative size of the nerve cords in *A. atropos* (Fig 5). Lateral and median intrinsic muscles are present throughout the entire proboscis but show differences in muscle arrangement and distribution. Median intrinsic muscle volume decreases from the proximal region to the tip whereas lateral intrinsic muscle volume displays a decrease from the proximal to the distal region but slightly increases within the tip region (Table 6). In proximal and distal proboscis regions, median intrinsic muscles display a larger volume and make up a larger percentage of the galea volume than lateral intrinsic muscles. Lateral intrinsic muscle volume only exceeds median intrinsic muscle volume within the tip region (Table 6). Muscular arrangement of lateral and median intrinsic muscles is only similar within the tip region. Here, lateral and median intrinsic muscles are each arranged in 3-4 muscle strands per cross-section (Fig 5d). Lateral intrinsic muscles progress dorso-laterally while median intrinsic muscles extend ventrally along the longitudinal axis of the galeae. In the distal and proximal regions of the proboscis, only the lateral intrinsic musculature consists of 2-4 individual muscle arrays per section. The median intrinsic musculature forms a compact muscular bundle positioned longitudinally along the ventral region of the galea (Fig. 5e, f). In the tip region, lateral muscle fibers show a mean length of 175 µm and extend in a mean angle of 26.95° (Table 4). Within the distal region, a lateral muscle fiber measures 118 µm in length and extends towards the dorso-lateral galea wall at approximately 32.2°. Proximal lateral intrinsic muscle fibers have a mean length of 99.2 µm and extend in a mean angle of 39.7° (Table 4). On average, lateral fibers are therefore shorter and extend at a steeper angle in proximal proboscis regions.

Table 4. Lengths and angles of lateral intrinsic muscle fibers from the proximal, distal and tip region in *A. atropos* (n=1) and *A. convolvuli* (n=1). For *A. atropos*, 3 fibers were measured. For *A. convolvuli*, 8 fibers were measured. Mean values were calculated only for *A. convolvuli*. "-" indicates inability to perform biometric measurements due to the structural anatomy of the musculature.

Region		***A. atropos***	***A. convolvuli***					**Mean (*A. conv.*)**
Tip	length (μm)	572	172	178				**175**
	angle	18.1°	26.1°	27.8°				**26.95°**
Distal	length (μm)	670	118					**118**
	angle	22.3°	32.2°					**32.2°**
Proximal	length (μm)	768	97	107	106	86	100	**99.2**
	angle	35°	47°	34.1°	38°	-	-	**39.7°**

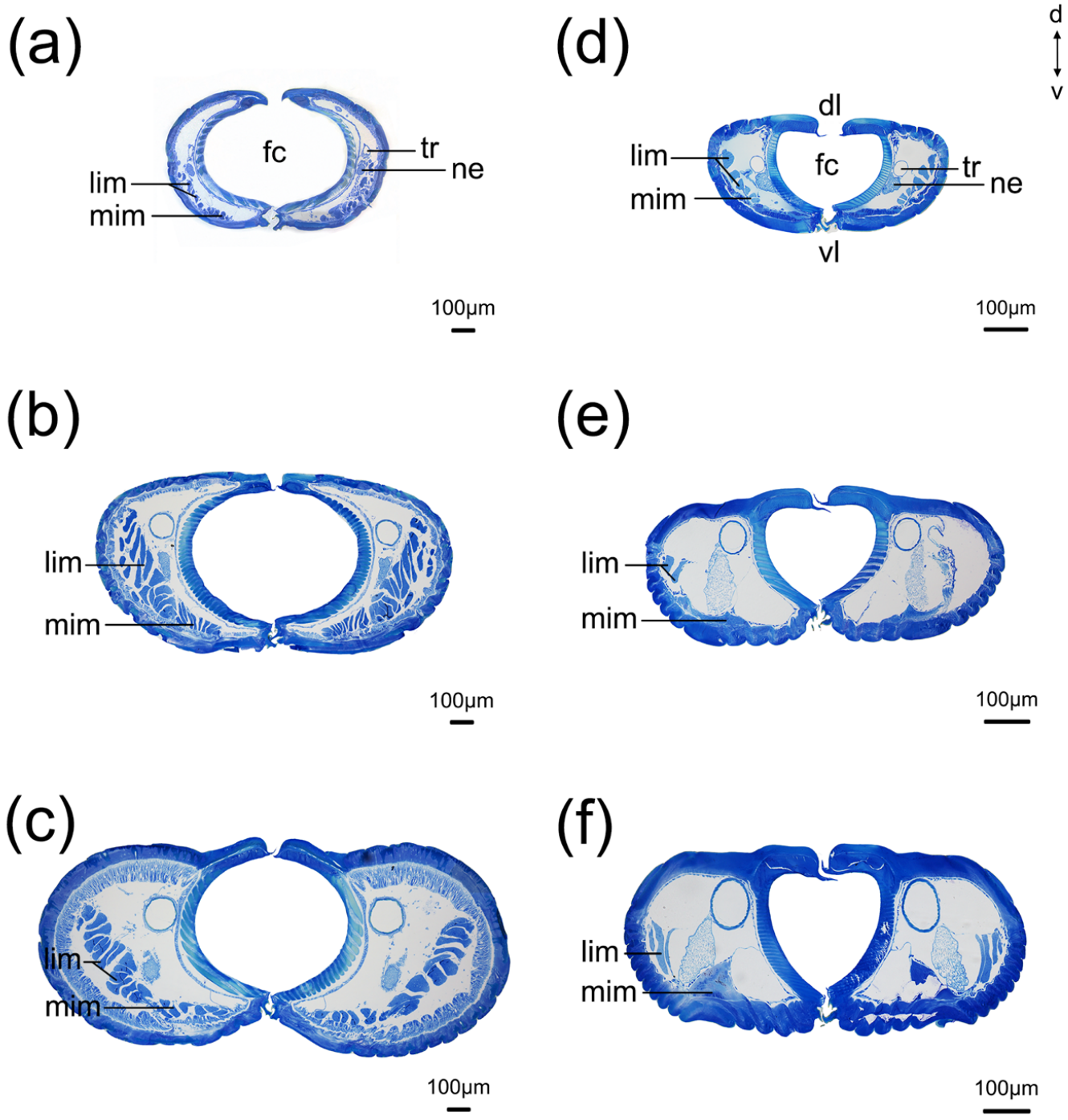

Fig. 5. Semithin sections of different proboscis regions in *A. atropos* (**a-c**) and *A. convolvuli* (**d-f**). **(a, d)** Tip region **(b, e)** Distal region **(c, f)** Proximal region. The food canal (fc) is enclosed by two galeae which are connected by dorsal (dl) and ventral legulae (vl). Dorsal leguale are only absent in the tip region of *A. atropos.* Tracheae (tr) and nerve cords (ne) extend throughout the proboscis. Lateral intrinsic muscles (lim) as well as median intrinsic muscles (mim) are present in all three proboscis regions of each species. d-v indicates the dorsoventral axis.

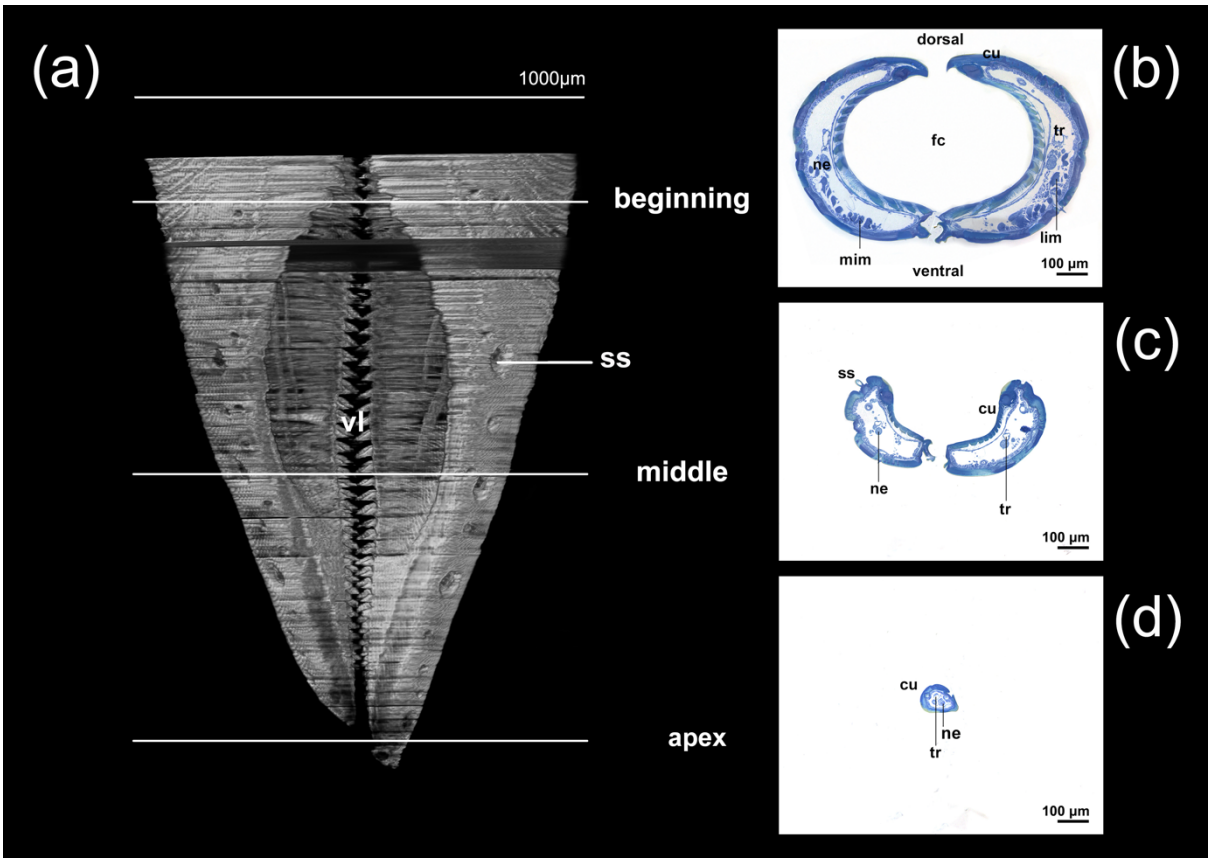

Fig. 6. Proboscis tip of *A. atropos.* **(a)** Volume rendering showing ventral legulae (vl) and sensilla styloconica (ss). Sensilla styloconica reach the apex of the tip. The opening of the food canal is elliptical and located subterminally. The food canal (fc) closes in the ventral galea region by interlocking of ventral legulae. **(b-d)** Cross sections from the beginning, middle and apex of the tip region exemplifying proboscis anatomy. Tracheae (tr), nerve cords (ne) and cuticula (cu) are found throughout the whole proboscis tip. Lateral intrinsic muscles (lim) und median intrinsic muscles (mim) do not extend into the apex of the tip.

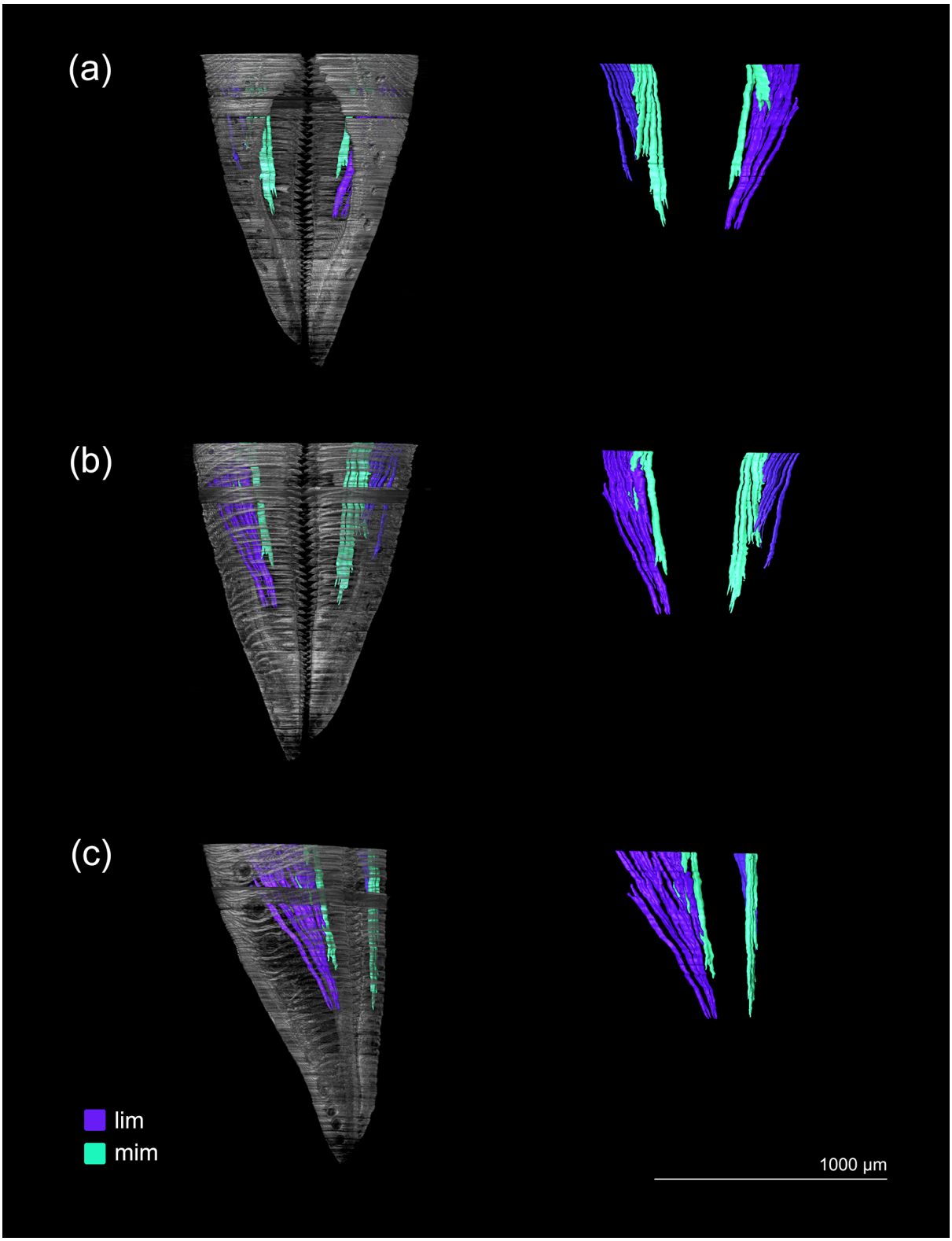

Fig. 7. Volume rendering of the proboscis tip and surface generation of the internal galea musculature (in colour) of *A. atropos*. **(a)** Dorsal view. **(b)** Ventral view. The distribution of lateral intrinsic muscles (lim) and median intrinsic muscles (mim) varies between the two galeae. Neither lim or mim extend fully into the apex of the tip. **(c)** Ventrolateral view. The lateral intrinsic musculature (lim) progresses dorso-laterally whereas the median intrinsic musculature (mim) extends longitudinally along the ventral axis of the galea.

The volume of the food canal, galeae, lateral intrinsic musculature and median intrinsic musculature displays noticeable differences between the short proboscid species *A. atropos* and the long proboscid species *A. convolvuli*. The volume of the food canal in the examined sections of the proboscis is 6 - 9 times larger in *A. atropos* than in *A. convolvuli,* depending on the proboscis region. This coincides with a more than 2.7 times larger food canal diameter in *A. atropos*. The galea volume of *A. atropos* is 2.5 – 5 times larger than the galea volume of *A. convolvuli* (Table 5). Here, the biggest size difference is found in the proximal proboscis region. Throughout all proboscis regions, lateral intrinsic muscle volume as well as median intrinsic muscle volume is substantially larger in *A. atropos*. Yet, the ratio of lateral intrinsic muscle volume$_{A.\ atropos}$: lateral intrinsic muscle volume$_{A.\ convolvuli}$ is very different depending on the proboscis region. Within the proximal proboscis region, lateral intrinsic muscle volume exhibits a ratio of 18 : 1, within the distal region, 35 : 1 and only 2.2 : 1 in the tip region. Only here, lateral intrinsic muscles of *A. convolvuli* even make up a larger percentage of the galea volume than in *A. atropos* (Table 6). Median intrinsic muscle volume (mim volume$_{A.\ atropos}$: mim volume$_{A.\ convolvuli}$) on the other hand, displays relatively even size ratios throughout the proboscis - with 2 : 1 in the proximal region, 4 : 1 in the distal region and 3.5 : 1 in the tip region. However, median intrinsic muscle volume of *A. convolvuli* makes up a larger percentage of the galea volume in the proximal galea region (Table 6). Muscle volume extrapolated to the entire proboscis length is more than 7 times larger in *A. atropos,* although *A. convolvuli* has a much longer proboscis (Table 6).

Table 5. Biometric / volumetric measurements of the proboscis, cuticula, food canal and galeae of the short proboscid *A. atropos* (n=1) and the long proboscid *A. convolvuli* (n=1). Volumetric values equate to 200 µm of the proximal, distal and tip region. The galea volume includes muscle volume.

	A. atropos	***A. convolvuli***
Proboscis length [mm]	12.4	70.5
Proboscis diameter [µm]		
Proximal	1950	827.5
Distal	1437	771
Tip	910	533.3
Cuticula width [µm]	80.3	59.2
Food canal diameter [µm]	655.6	236.6
Food canal volume [mm^3]		
Proximal	0.06	0.008
Distal	0.06	0.007
Tip	0.04	0.007
Galea volume (left; right) [mm^3]		
Proximal	0.11; 0.13	0.02; 0.02
Distal	0.07; 0.07	0.018; 0.019
Tip	0.02; 0.02	0.008; 0.008

Table 6. Volumetric measurements of the internal galea musculature (lim and mim) of the short proboscid *A. atropos* (n=1) and the long proboscid *A. convolvuli* (n=1). Volumetric values equate to 200 µm of the proximal, distal and tip region unless otherwise specified. lim – lateral intrinsic muscles, mim – median intrinsic muscles

Internal Galea Musculature	*A. atropos*	*A. convolvuli*
Lim volume (left; right) [mm³]		
Proximal	0.008; 0.008	0.0005; 0.0004
Distal	0.007; 0.007	0.0002; 0.0002
Tip	0.0009; 0.0004	0.0003; 0.0003
[% of galea volume]		
Proximal	6.7	2
Distal	10.1	1
Tip	3	3.6
Mim volume (left; right) [mm³]		
Proximal	0.002; 0.002	0.001; 0.001
Distal	0.002; 0.002	0.0006; 0.0004
Tip	0.0003; 0.0004	0.0001; 0.0001
[% of galea volume]		
Proximal	1.7	4
Distal	2.9	2.7
Tip	1.7	1.2
Projected muscle volume, entire proboscis [mm³]	4.55	0.6

3.2.2 Basal Galea Musculature and Stipes Pump

In both species, basal galea muscles are found within the proximal proboscis region. They form a prominent muscle group located closely to the stipes pump. Thereby, the muscle arrangement is the same in *A. atropos* and *A. convolvuli*. The basal galea musculature extends from the proximal base of the galea to the dorsal proboscis wall (Fig 8, 10a, d). Especially towards the dorsal attachment point, the basal galea musculature in *A. atropos* is broader and more massive than in *A. convolvuli*. This is supported by a larger basal galea muscle volume in *A. atropos* (Table 7). The two muscles composing the basal galea musculature show a low level of distinctiveness within both species. However, two muscles are visible in *A. atropos*. Here, the median muscle displays longer muscle fibers. The other muscle progresses laterally alongside the median muscle and attaches to the dorsolateral galea wall. In *A. convolvuli*, no such distinction can be made (Fig 8).

The structural composition and muscular arrangement of the stipes pump are the same in the short proboscid species *A. atropos* and the long proboscid species *A. convolvuli*. Two principal muscle groups are found: the internal stipes muscle and the external stipes muscles. The latter consists of two distinct muscles which differ in origin and attachment points. The external stipes muscle 1 (*musculus clypeo-stipitalis*, Krenn & Bauder 2017) originates on the clypeus, progresses laterally past the anterior tentorium and attaches to the lateral stipes sclerite via a tendon (Fig 9). It consists of two distinct muscles and is therefore divided. This separation is clearly visible in *A. convolvuli* but only inconspicuous in *A. atropos* (Fig 9). The external stipes muscle 2 (*musculus tentorio-stipitalis externalis*, Krenn & Bauder 2017) originates on the ventral side of the tentorium, medially of the *musc. clyp. stip.*, and attaches to the flat stipes sclerite. The internal stipes muscle (*musculus tentorio-stipitalis internalis*, Krenn & Bauder 2017) on the other hand, originates at the posterior tentorium and extends almost longitudinally to the anterior, median part of the stipes (Fig 9).

In both species, external stipes muscles are larger than internal stipes muscles. Therefore, external stipes muscles make up 4 % of the head capsule volume while internal stipes muscles make up approximately 1 % (Table 7). External stipes muscle volume as well as internal stipes muscle volume is only slightly larger in *A. convolvuli* (3.8; 0.9 mm^3) compared to *A. atropos* (3.2; 0.8 mm^3). This is matched by a larger head diameter and a larger head capsule volume in *A. convolvuli* (Table 7).

Table 7. Volumetric / biometric measurements of the basal galea musculature, head capsule and stipes muscles analyzed in *A. atropos* (n=1) and *A. convolvuli* (n=1). Head capsule volume includes the complex eyes, the external and internal stipes muscles, but not the basal galea muscles. External stipes muscle volume includes external stipes muscles 1 and 2.

	A. atropos	***A. convolvuli***
Basal galea muscle volume (mm^3)	0.2	0.14
Head capsule diameter (mm)	8	8.3
Head capsule volume (mm^3)	81	93.7
Stipes pump		
External stipes muscle volume (mm^3)	3.2	3.8
[% of head capsule]	4	4
Internal stipes muscle volume (mm^3)	0.8	0.9
[% of head capsule]	1	1

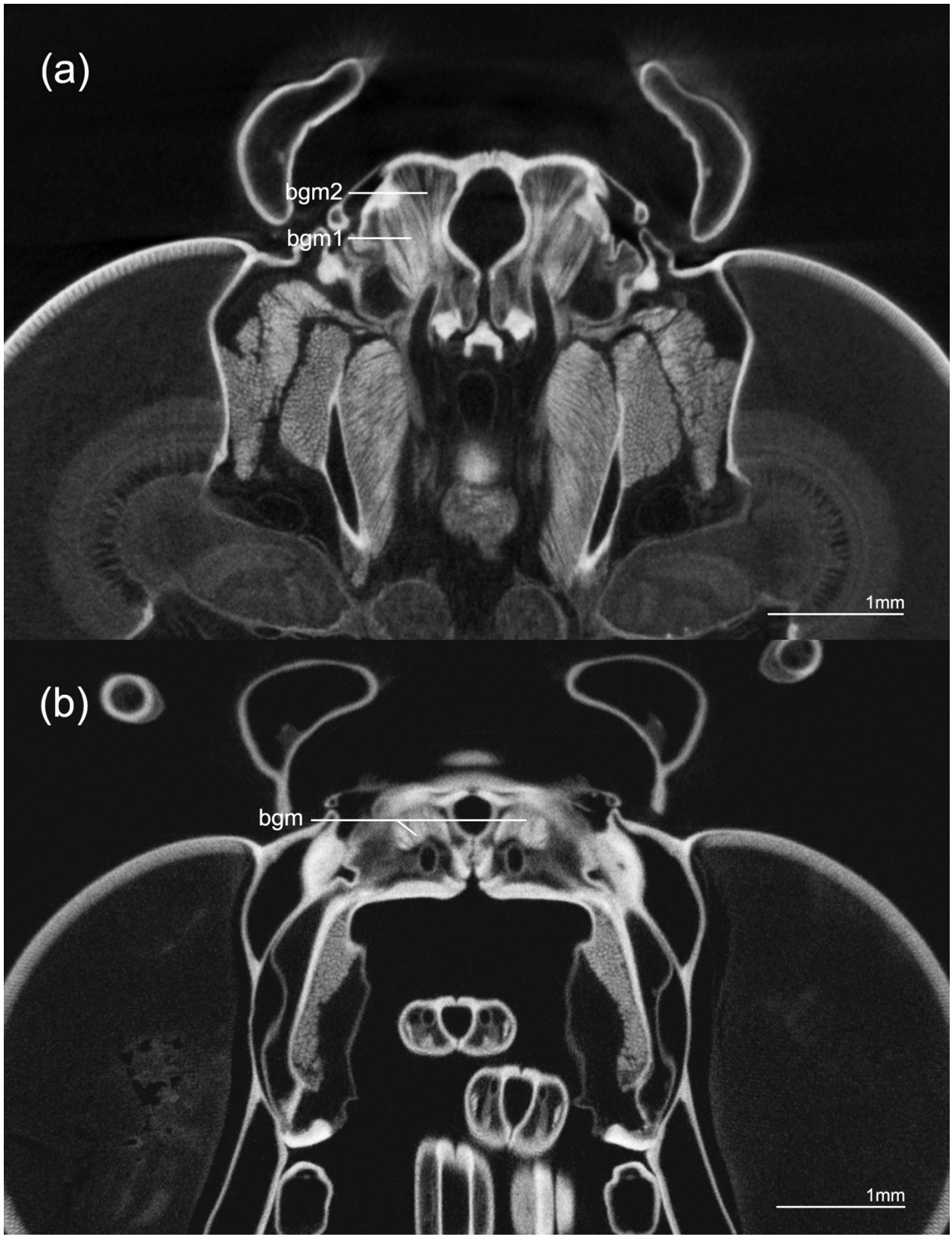

Fig 8. Anatomy of the basal galea musculature of the short proboscid species *A. atropo*s **(a)** and the long proboscid species *A convolvuli* **(b)** (MicroCT). Transverse section of the heads. Basal galea muscles (bgm) in both species originate at the stipes-galea junction and attach to the dorsal / dorsolateral proboscis wall. Two distinct basal galea muscles are distinguishable in *A.atropos*. Here, the median basal galea muscle (bgm2) displays longer muscle fibers than the medio-laterally positioned basal galea muscle (bgm1). The basal galea musculature of *A.atropos* is larger and structurally more defined than the basal galea musculature of *A. convolvuli.*

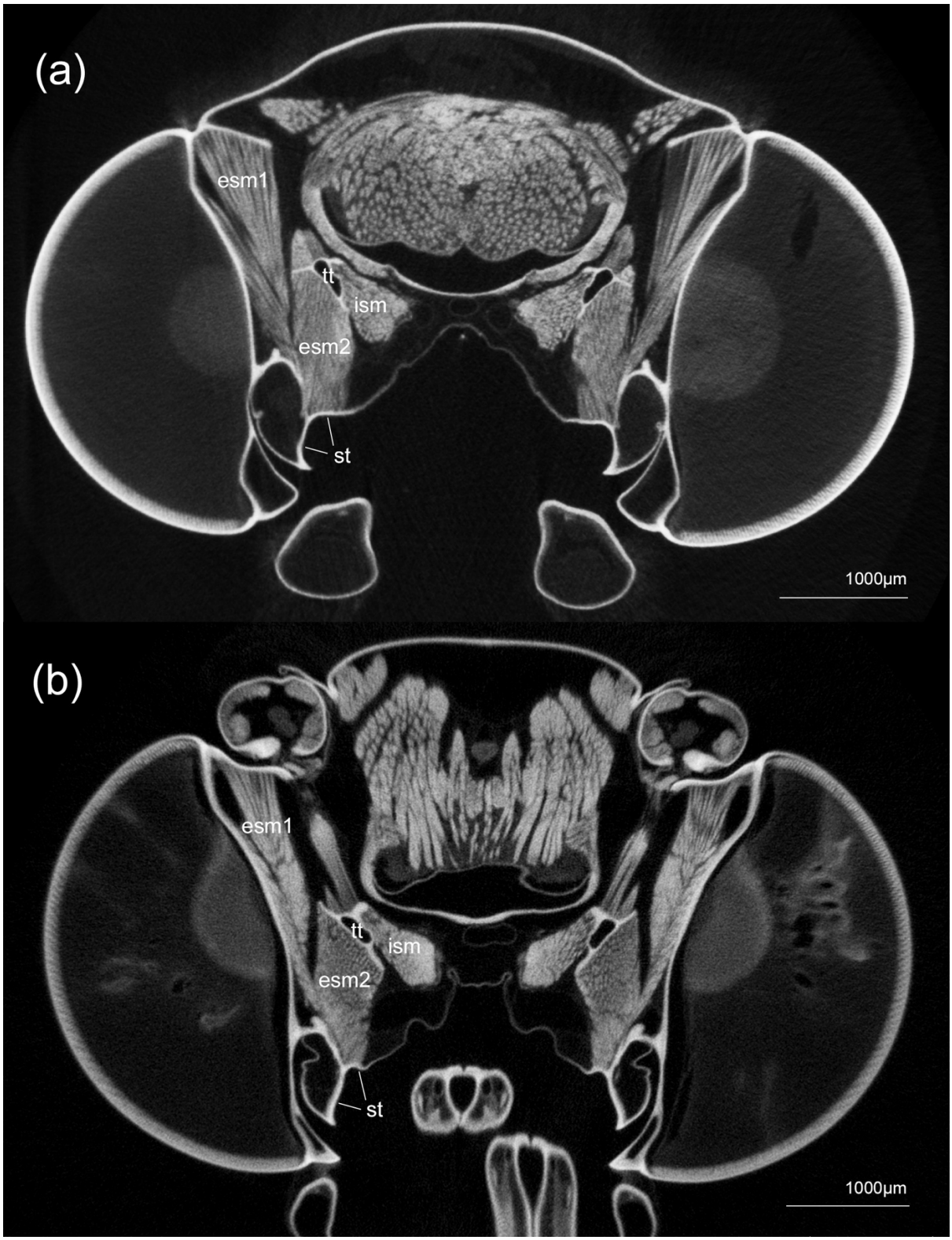

Fig 9. Anatomy of the stipes pump of **(a)** the short proboscid species *A. atropo*s and **(b)** the long proboscid species *A convolvuli* (MicroCT). Cross section of the heads. Muscular arrangement and principal composition of the stipes pump are the same in both species. The stipes pump consists of a lateral pointed sclerite, a medial flat sclerite and compressor muscles. Compressor muscles consist of the external stipes muscle 1 (esm1), the external stipes muscle 2 (esm2) and the internal stipes muscle (ism). The esm1 originates on the clypeus and attaches to the stipes sclerite (st). A separation between the esm1 muscles is clearly visible in *A. convolvuli* but barely detectable in *A. atropos*. The esm2 originates at the ventral tentorium (tt) and extends towards the flat stipes sclerite (st). The ism progresses longitudinally along the tentorium up to the median anterior part of the stipes.

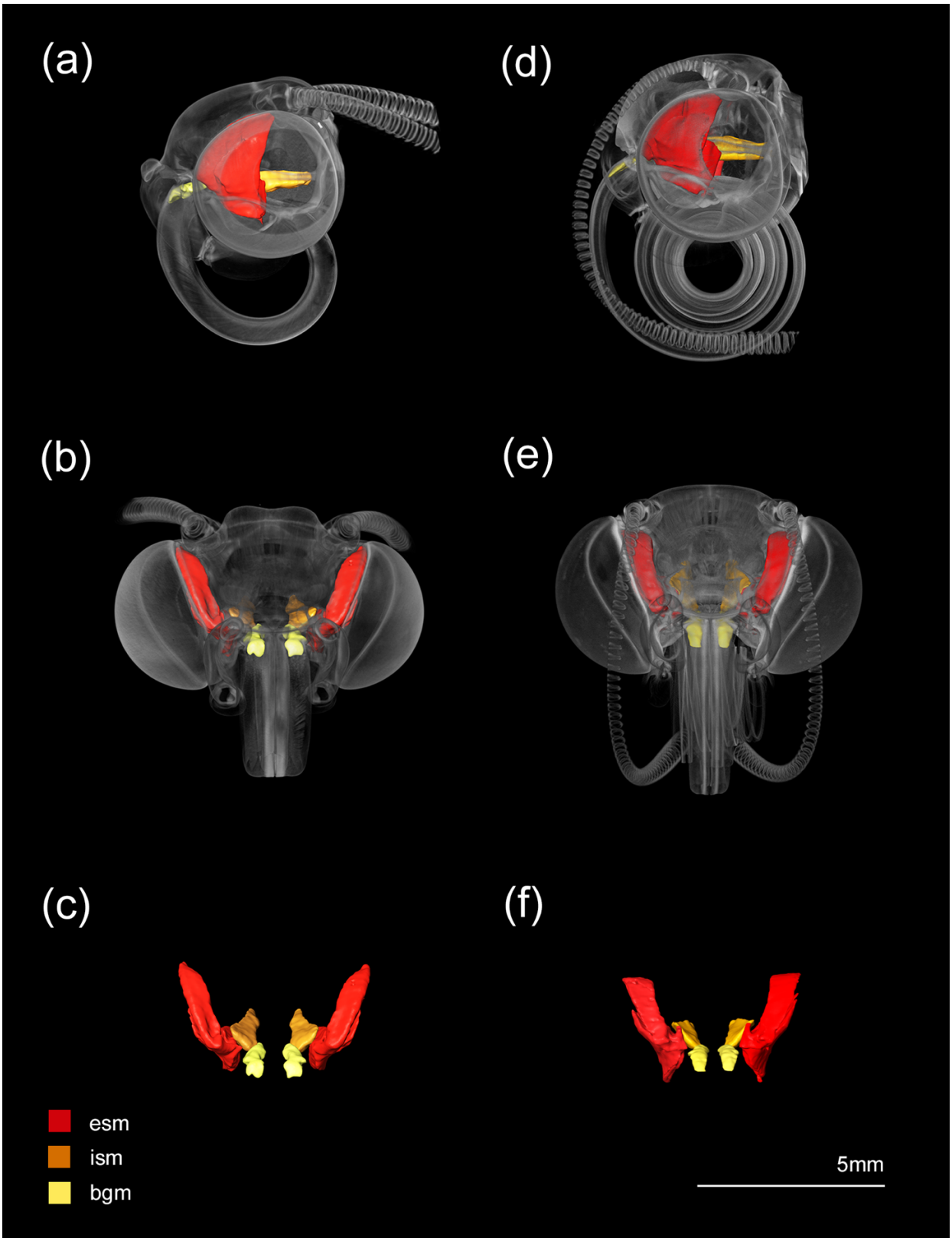

Fig 10. Head of the short proboscid *A. atropos* **(a-c)** and long-proboscid *A. convolvuli* **(d-f)** (MicroCT). Surface generation of the stipes pump and basal galea musculature in colour. **(a, d)** Lateral view. **(b, e)** Anterior view. **(c,f)** Stipes muscles and basal galea muscles without the head capsule. Anterior view. External stipes muscles (esm) and internal stipes muscles (ism) originate at the head capsule or tentorium and attach to the stipes. Esm are larger and more prominent than ism. Basal galea muscles (bgm) originate at the galea base and attach to the dorsal proboscis wall.

4. Discussion

4.1 Proboscis Morphology

4.1.1 Proboscis Length and Shape

Several differences in proboscis morphology between *A. atropos* and *A. convolvuli* were found. Especially the great disparity in proboscis length between the two species is obvious. The proboscis of *A. atropos* is substantially shorter than the proboscis of *A. convolvuli*. Considering the different feeding strategies of these two species, this may be attributed to an adaptation relating to foraging behavior and feeding preference. As stated by multiple authors, most adult Lepidoptera feed primarily on floral nectar using a more or less long proboscis formed by the maxillary galeae (Krenn et al. 2001; Krenn 2010; Mitter et al. 2017). In conjunction, many flower-visiting species are equipped with a long proboscis which enables them to reach nectar inside deep-throated flowers (Krenn 2008; Krenn 2010; Lehnert et al. 2016). Particularly Sphingidae are known for their long proboscises and hovering flight in front of flowers during nectar feeding (Stöckl & Kelber 2019). The longest proboscises recorded so far, have been found in the sphingids *Amphimoea walkeri* (Boisduval, 1875), *Xanthopan morganii praedicta* (Walker, 1856) and several *Cocytius* species (Amsel 1938, Netz & Renner 2017). Thereby, the proboscis of *A. walkeri* may measure up to 28 cm while the proboscis of *Neococytius cluentius* (Cramer, 1776) measures about 25 cm (Amsel 1938; Faucheux 2013). The proboscis of *X. morganii praedicta* is around 21.7 ± 0.42 cm long (Wasserthal 1997). Although not among the record holders in proboscis length, the flower-visiting species *A. convolvuli* possesses a rather long proboscis, which is designed for finding and extracting nectar. In the studied specimen, the proboscis measured about 7 cm, records of other individuals however, documented proboscis lengths of about 14 cm for this species (Nilsson et al. 1985). In contrast, the short proboscis in *A. atropos* is most likely an adaptation to the species´ way of obtaining honey inside the beehives. The length of the proboscis matches the depth of the honeycombs, which are typically 1.25 - 1.77 cm deep (Hüsing & Nitschmann 1987). A short and robustly built proboscis may be crucial when piercing through the waxy seals of honeycombs. It is also intuitively obvious that a long proboscis may inconvenience the adult moths inside the beehive as there is only limited space. Furthermore, a long proboscis may impede the generation of the force adequate for penetrating the seals of the honeycombs. Interestingly, males of the blood-sucking moth *Calyptra eustrigata* (Noctuidae) (Hampson, 1926), which have been found to pierce fruit as well as the skin of humans or even ungulates and elephants (Bänziger, 1968,

1980), display a similarly short proboscis (Fig 11b). This is further supported by records of the blood-feeding moth *Calyptra thalictri* (Borkhausen, 1790) (Bänziger 1970; Fig 11a), findings of stout proboscises in fruit-piercing Charaxinae (Krenn et al. 2001) and other noctuids (Faucheux 2013). Therefore, piercing behavior in many Lepidoptera seems to be related to a reduction of proboscis length relative to body size. This is also the case in other blood-feeding insects (Krenn & Aspöck 2012). As stated by Krenn & Aspöck (2012), the typical piercing proboscis of a blood-consuming insect is usually relatively short compared to the proboscis of a nectar-feeding species.

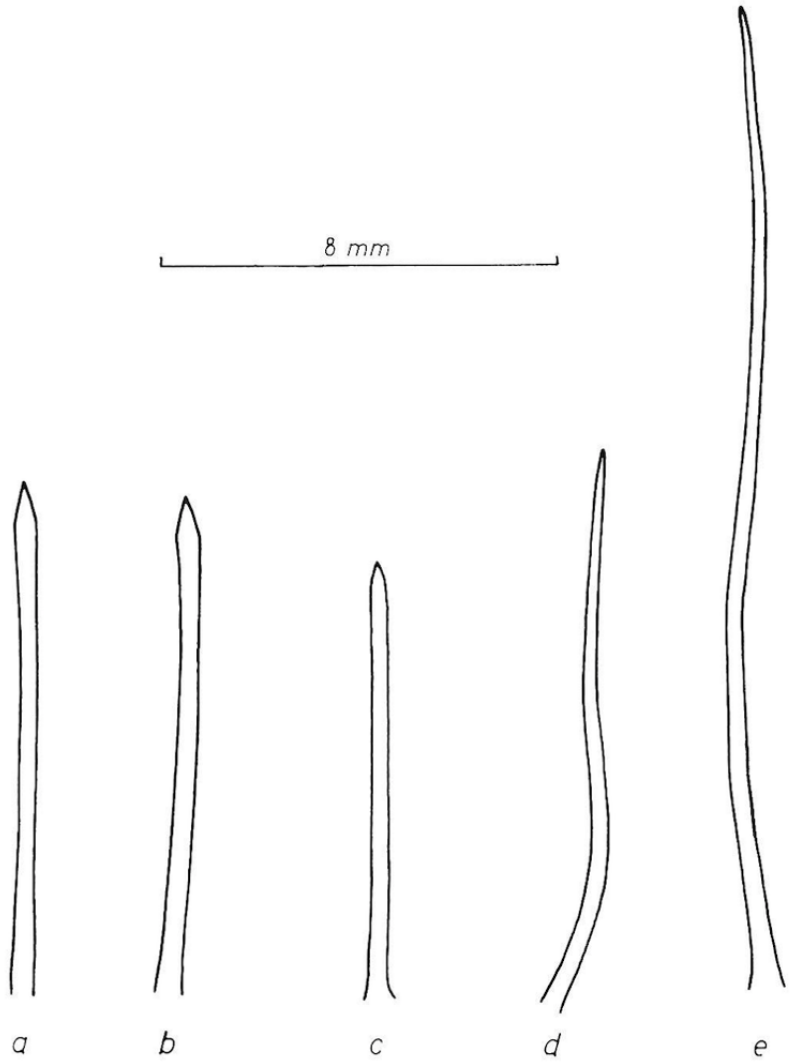

Fig. 11. Proboscis dimensions of some noctuid moths. (**a)** *Calyptra thalictri* (fruit-piercing). (**b)** *Calyptra eustrigata* (skin-piercing, blood-sucking). **(c)** *Scolyopteryx libatrix* (Linnaeus, 1758) (fruit-piercing). **(d)** *Lygephila craccae* (Denis & Schiffermüller, 1775) (non-piercing, fruit-sucking). **(e)** *Autographa gamma* (Linnaeus, 1758) (nectar-sucking). Figure from Bänziger 1970.

4.1.2 Proboscis Tip

The apical drinking region in *A. atropos* and *A. convolvuli* displays noteworthy morphological differences. Generally, morphological variations of the proboscis tip attributed to specialized feeding strategies are well studied in Nymphalidae, Erebidae, Noctuidae and others (Krenn et al. 2001; Zaspel et al. 2011; Zenker et al. 2011). In sphingids however, functional interpretations of varying tip morphologies aren't as present. This may be partially due to their prevalent function as flower pollinators throughout their geographical distribution (Haber & Frankie 1989; Powell 2009). As a nectar feeder, the long proboscid *A. convolvuli* exhibits many adaptations typically associated with these flower-visiting species. The slender tip is characterized by prominent drinking slits for nectar consumption as is described in many other nectar-consuming Lepidoptera (Krenn 2010; Lehnert et al. 2016). The distinct proboscis tip morphology in *A. atropos* on the other hand, is unique within the Sphingidae and even the entire lepidopteran order. The tip is smooth and sharply pointed while displaying a large opening of the food canal. Although pointed proboscis tips can also be found in certain fruit-piercing or blood-feeding moths, their morphology is noticeably different from the tip of *A. atropos*. In blood-sucking species such as *C. eustrigata,* the proboscis displays a conoid, stiff point which may be heavily sclerotized (Bänziger 1980). In fruit-piercers such as *C. thalictri* or *S. libatrix,* a sudden, almost triangular pointing of the proboscis tip is noticeable (Bänziger 1970). However, the tips of these fruit-piercing or blood-sucking species display prominent tearing hooks, erectile barbs and / or rasping spines (Bänziger 1970; 1980; Zaspel et al. 2011; Fig 12a-c) which are not present in *A. atropos*. The smooth cuticular surface of the tip in *A. atropos* therefore shows a greater resemblance to that of a nectar-feeding species (Fig 12e).

Fig 12. Distal part of the proboscis and armature of some noctuid moths exhibiting different feeding modes. **(a)** *Calyptra thalictri* (fruit-piercing). **(b)** *Calyptra eustrigata* (skin-pericing, blood-sucking). **(c)** *Scolyopteryx libatrix* (fruit-piercing). **(d)** *Lygephila craccae* (non-piercing, fruit-sucking). **(e)** *Autographa gamma* (nectar-sucking). Figure from Bänziger 1970.

The subterminal, elliptical opening of the food canal recorded in *A. atropos* has not yet been discovered in other Lepidoptera. It is likely that this morphology of the apical drinking region resembles another adaptation to the moth´s feeding mode, but it may also be related to sound production. Yet, the latter is unclear. In context with piercing however, an opening such as this is postulated to provide stability while preventing blockages of the canal (Foelix 2011). Again, this is probably beneficial when piercing the waxy seals of the honeycombs and has further

been found in various substance-piercing structures across multiple animal taxa. Presumably, as the outcome of a process of natural selection, the chelicerae of spiders, the stingers of scorpions and fangs of venomous snakes have all convergently developed identically structured tips and openings (Foelix 2011; Zhao et al. 2016; Du Plessis et al. 2018; Fig. 13 b-d). Likewise, hypodermic needles, which are applied in human medicine, are fabricated with an elliptical, subterminal opening and a tapered tip (Huber 1946; Fig 13a).

From a mechanical point of view, such tapered, slightly bent structures attain maximum stress in the near-tip region upon penetration and consequently provide exceptional load-bearing capabilities. Therefore, this structural design, along with a subterminal, elliptical opening of the canal, proves to be a common solution in liquid-injecting or extracting structures (Bar-On 2019). Within the Lepidoptera however, this tip morphology is only found in *A. atropos*.

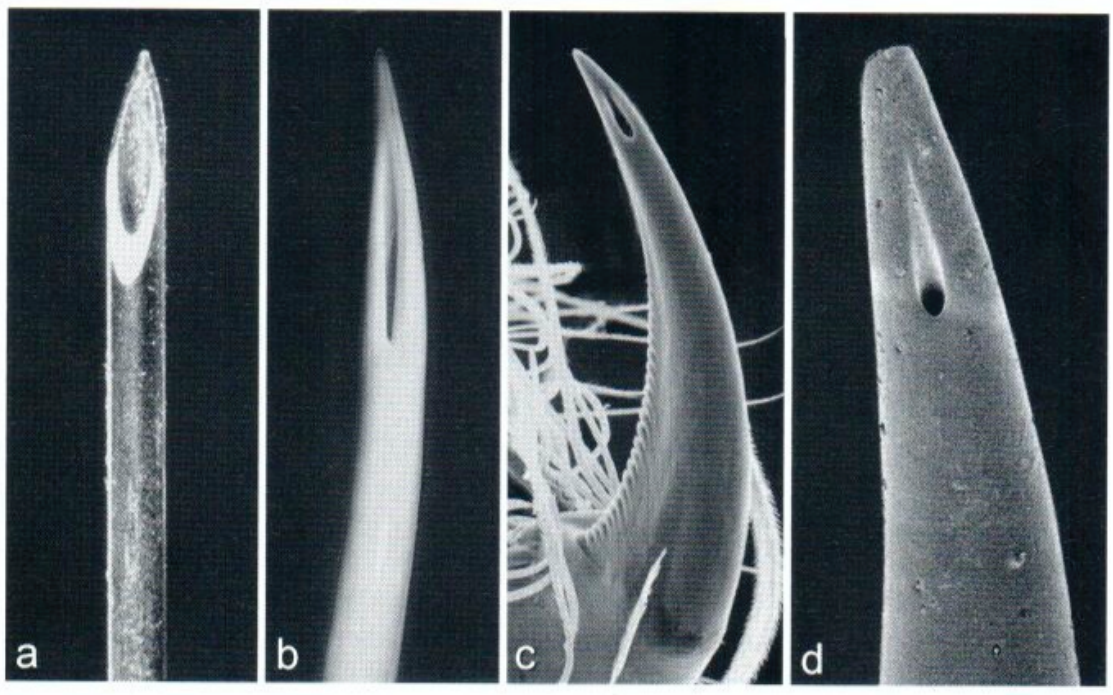

Fig. 13. Structures containing an elliptical, subterminal opening for improved drug or venom injection **(a)** Hypodermic needle **(b)** Venom tooth of a viper **(c)** Cheliceral fang of a spider, **(d)** Stinger of a scorpion (Photos from Foelix and Erb.). Figure from Foelix 2011.

4.1.3 Sensilla and Cuticula

The sensilla equipment of *A. atropos* and *A. convolvuli* is relatively uniform and shows slight variation only in distribution and relative sensilla amount. Structurally, s. trichodea, external s. basiconica and s. styloconica only show minor differences in size. These findings stand in contrast to highly variable sensilla types in context with specialized feeding preferences in

groups such as Nymphalidae and Noctuoidea (Krenn et al. 2001; Zaspel 2008; Pinterich & Krenn 2020). However, certain sensilla types, such as s. trichodea and s. basiconica, are highly preserved throughout all lepidopteran superfamilies (Faucheux 2013). As their mechanoreceptive function has been widely accepted (Gnatzy & Tautz 1980; Bauder et al. 2011; Faucheux 2013), s. trichodea perceive tactile stimuli throughout the entire proboscis. In nectar feeders, apical s. trichodea are responsible for detecting the opening of corolla tubes (Bauder et al. 2011). Sensilla spread over the length of the proboscis are said to inform the lepidopteran on corolla diameter as well as proboscis insertion depth (Faucheux 2013). In Sphingidae specifically, slender s. trichodea are rather inconspicuous and only barely protrude above the galea surface (Faucheux 2013), which is the case in *A. atropos* as well as *A. convolvuli*. This seems to be especially important in the piercing proboscis of *A. atropos*, as long sensilla may hinder its´ insertion into the honeycombs. As an exception, s. trichodea are reported to be very long in the sphingid *Macroglossum stellatarum* (Linnaeus, 1758), which collects nectar during flight (Faucheux 2013).

Although external s. basiconica are also found in all Lepidoptera, they are small and inconspicuous in many species, such as *A. atropos* and *A. convolvuli*. According to Faucheux 2013, s. basiconica are partially replaced by s. styloconica in higher families. Therefore, s. basiconica may become rarer without fully disappearing. In species with no s. styloconica, s. basiconica can be found in large numbers (Faucheux 2013). Due to their ultrastructure, s. basiconica are regarded as contact chemosensilla (Krenn 1998). Depending on their positioning on the proboscis, they are stimulated at first contact with the food source or after deeper insertion of the galeae into the liquid (Faucheux 2013). Since s. basiconica are found even at the apex of the proboscis tip in *A. atropos*, they are likely to give the moth clear information on whether it has reached the honey inside the combs or not. Internal s. basiconica on the other hand, give information about liquid flow and quality (Faucheux 2013). They are positioned along the inner wall of the food canal, which is composed very similarly in all Lepidoptera (Faucheux 2013).

From an evolutionary point of view, the first presence of bimodal taste / tactile s. styloconica among Lepidoptera is disputed by different authors (Krenn & Kristensen 2000; Faucheux 2007) and they are further absent in families such as the Tineidae (Faucheux 2013). Electrophysiological studies have revealed a response of s. styloconica to amino acids as well as mono- and oligosaccharids (Salama et al. 1984; Blaney & Simmonds 1988). Just as in *A. atropos* and *A. convolvuli*, they are present only in the most distal regions, particularly in the

area where the fluid is sucked in. Here, they supposedly help localize the opening of the flower and the nectar inside the corolla (Faucheux 2013). The number and morphology of s. styloconica often varies greatly with feeding preference (Krenn et al. 2001; Faucheux 2013; Lehnert et al. 2016). Compared to nectar-feeding species, lachryphagous species often display fewer s. styloconica (Faucheux 2013). But even nectivorous Riodinidae are often characterized by a small number of short sensilla (Bauder et al. 2011; Bauder et al. 2013). In non-flower visiting nymphalids, s. styloconica are highly diverse. Especially long s. styloconica in high densities are found in non-flower visiting Satyrinae, Apaturinae, Nymphalinae and others (Krenn et al. 2001). In these species, they form a flat brush at the tip of the proboscis. This is typically associated with the intake of free fluids, tree sap or decaying fruit. Proboscises of representatives of the Charaxinae on the other hand, display rather short sensilla styloconica, similarly to *A. atropos*. It has been observed that these species can pierce the skin of decaying or squashy fruit (Krenn et al. 2001).

In addition, many fruit- or skin-piercing Lepidoptera can move their galeae independently. In *C. thalictri*, perforation of the skin is achieved by an antiparallel movement of the left and right galea, driven by the protractor and retractor muscles. The sawing motion enables the tearing structures of the galeae to tear a hole big enough for the proboscis to fit through (Bänziger 1970). Similarly performing mouthparts have been found in other blood-feeding insects as well (Krenn & Aspöck 2012). The galeae of *A. atropos* however, are interlocked and not capable of interchangeable, rasping motions. Therefore, the proboscis is forced into the wax with shear force. This piercing mechanism separates *A. atropos* from other piercing moths and is very likely only applicable for the penetration of soft materials, such as wax.

Many fruit- or skin-piercing species, such as *C. eustrigata* and *C. thalictri*, also display a highly specialized armature of the proboscis. It is equipped with prominent hooks, barbs, teeth, spines and / or others. In *C. eustrigata*, *C. thalictri* and *S. libatrix* specifically, slender erectile barbs are found. These most likely evolved from s. styloconica (Bänziger 1970; Büttiker et al. 1996). In an extended proboscis, they can be actively erected by an increase in blood pressure and therefore assist the piercing mechanism (Bänziger 1970). However, the proboscis of *S. libatrix* and many fruit-licking Noctuidae, lacks tearing hooks. As previously mentioned, this is also the case in *A. atropos,* as this species displays only short sensilla and no specialized armature of the proboscis. In conclusion, highly specialized sensilla or cuticular armatures may not be necessary for the successful piercing of honeycombs and the intake of honey.

However, the proximal galea region of *A. atropos* and *A. convolvuli* displays long hair-like

sensilla. These have reportedly already been observed in *A. atropos* but not in other Sphingidae, such as *A. convolvuli* (Faucheux 2013). According to other authors, these long sensilla are mechanoreceptive (Altner et al. 1983) and are sensitive to air currents or low-frequency sounds in insects (Gnatzy & Tautz 1980; Faucheux 2013). Apparently, these sensilla are responsible for the localization of approaching guard bees and triggering a flight response in *A. atropos* (Faucheux 2013). This is yet to be confirmed by behavioral studies. In *A. convolvuli*, the long bristle shaped sensilla may measure corolla diameter or warn the moth about incoming predators. However, additional data is necessary to make conclusive assumptions about their possible function in this species.

All in all, the similar sensilla morphology and distribution of *A. atropos* and *A. convolvuli* supports a rather uniform sensilla micromorphology within the Sphingidae, as opposed to other species with derived feeding preferences found in the Nymphalidae and Noctuoidae. Regardless of a highly specialized lifestyle in *A. atropos*, a more general sensilla structure, also found in *A. convolvuli,* is present. This may indicate that no specialized sensilla morphology is required for piercing honeycombs.

4.2 Proboscis Anatomy

4.2.1 Food Canal & Biomechanics of Honey Consumption

The large diameter and volume of the food canal in *A. atropos*, especially when compared to its´ flower-visiting relative *A. convolvuli*, can be interpreted as an adaptation for feeding on honey and for counteracting the low flow rate caused by viscous fluids. As described by the Hagen-Poiseuille law, the flow rate (V) of a fluid is proportionate to the radius to the power of four (r^4) of the construct it is moving through. Enlargement of the food canals ´ radius therefore results in a much larger fluid uptake capacity within the same period of time. Fluid viscosity (η) and proboscis length (l) on the other hand, are inversely related to flow rate. With honey presumably having a higher level of viscosity, it affects the flow rate negatively. To account for this, the food canal diameter of *A. atropos* is enlarged while the proboscis is relatively short compared to *A. convolvuli* or other Lepidoptera specializing in nectar intake (Kitching 2003).

$$V = \frac{dV}{dt} = \frac{\pi \cdot \mathrm{r}^4}{8 \cdot \eta} \frac{\Delta \mathrm{p}}{l}$$

Typically, the viscosity of honey-like substances is estimated at 351–1750 centipoise (cP), fluids with a viscosity of 51–350 cP are categorized as nectar-like liquids (Garcia et al. 2005). However, the viscosity of honey may vary with geographical location and flora (Naheed & Farooqi 2018). It is also affected by water content and temperature (Lipp 1994). According to Oroian (2013), the viscosity of honey decreases with increasing temperature. At 39.4°C, a viscosity of 2100 cP was recorded for sweet clover (*Melilotus*) honey with a water content of 16.1 %. At 29°C the same honey had a viscosity of 6800 cP. For sage (*Salvia*) honey with a water content of 18.6%, a viscosity of 5500 cP was documented at 30.7°C (Lipp 1994). This temperature approximately corresponds the conditions found inside beehives, as the colony typically tries to keep the temperature close to 33 – 36°C (Kridi et al. 2014). However, these results were given in Pascal second (Pa*s) by Lipp (1994), and the conversion to cP yielded very high values. Also, the exact viscosity of the honey inside the honey cells is unknown. Reports further suggest that the honey inside the combs is inhomogeneous, which in turn may indicate that the viscosity may vary even within the same cell (Eyer et al. 2016).

In captivity, it has been observed that adult *A. atropos* individuals are not able to pull store-bought honey, even if it is preheated to approximately 36°C (Manuel Staggl BSc, personal observation). Yet, it is known that beekeepers dehydrate honey after removing it from the beehive, which in turn causes it to thicken. Typically, honey with a water content above 19% is not suitable for distribution, as there is an increased risk of fermentation (Mag. Med. Vet. Philipp Maier, personal statement). Moths fed with honey-water recognize mixtures with a ratio of 1 : 1 (estimated viscosity of sunflower-oil) as food, mixtures with lesser honey quantities are rejected. Mixtures with a honey to water ratio of 1.5 : 1 can be sucked-up through the proboscis by larger individuals. Any mixture with a greater honey content is accepted by the moths but cannot be pulled up through the proboscis (Manuel Staggl BSc, personal observation). It is further important to mention, that bees ripen the honey inside the hive. After the nectar is ingested and regurgitated multiple times, it is filled into the honeycombs. The worker bees then remove excess water by fanning the honey with their wings (Abdallah 2014). The loss of water causes the honey to thicken and the sugar concentration to rise. Eyer et al. (2016) have suggested, that cell capping is also a part of the ripening process and that the sugar concentration rises even further once the cell is sealed. Sugar concentrations may reach up to 80% once the honey is fully ripe (Park 1933). Thus, unripe honey is less viscous than ripe honey. Speculations may therefore suggest that adult *A. atropos* specimens only drink from combs containing honey with low sugar concentrations. However, observations have

confirmed that *A. atropos* also drinks from sealed honeycombs, invalidating this theory. It is possible that moths may regurgitate saliva into the honeycombs to dilute the honey. Yet, this is not confirmed by Manuel Staggl BSc, who has not noticed this behavior in captive individuals. Therefore, monitoring wild individuals during feeding would be necessary for making further conclusions on this subject. Furthermore, measuring the honey viscosity in different cells, as well as different positions within the same cell, would be beneficial for understanding the feeding mechanism of *A. atropos*.

It has also been suggested that the pressure drop (Δp; see Hagen-Poiseuille law) produced by the sucking pump correlates positively with the flow rate of the liquid passing through the food canal (Krenn 2010). Yet, additional data would be required to make conclusive assumptions about the pressure produced by the suction pump of *A. atropos*. Kornev et al. (2017) however, have already suggested that *A. atropos* only invests little muscular energy in combating viscous drag when moving fluids through the proboscis. They further note that viscosity alone is not the sole determinant of the muscle strength required to move the liquid through the proboscis. Additionally, it is stated that the muscular development of the suction pump in *A. atropo*s and *Manduca sexta* (Linnaeus, 1763) (Sphingidae) is similar and that the pump chambers are theoretically interchangeable without compromising *A. atropos´* ability to pull honey inside the beehives (Kornev et al. 2017).

4.2.2 Internal Galea Musculature

Lateral and median intrinsic muscle arrangements inside the proboscis differ between *A. atropos* and *A. convolvuli*. This is especially obvious in the proximal and distal proboscis regions. Furthermore, lateral intrinsic muscles make up a larger percentage of the galea volume than median intrinsic muscles in *A. atropos*. In *A. convolvuli*, this is only the case in the tip region. Muscular angles of slope are steeper in *A. convolvuli*. Lateral muscle fibers in both species display the flattest muscular angles of slope in the tip region and the steepest angles of slope in the proximal galea region. It is important to note however, that the measurements were only performed on one individual per species. Results are therefore not quantitatively valid. Although it is well known that both, lateral and median intrinsic muscles, are involved in proboscis recoiling (Krenn 2000; Krenn & Mühlberger 2002; Wannenmacher & Wasserthal 2003), an exact functional differentiation between the two muscle groups has not been made so far. Unfortunately, this is also the case for functional diagnoses of different muscular angles

of slope in Lepidoptera. Therefore, functionally interpreting the differing muscular traits in *A. atropos* and *A. convolvuli* is not possible yet. The analyses of lateral intrinsic muscles, median intrinsic muscles and different muscular angles in a functional context should therefore be further investigated.

Absolute lateral and median intrinsic muscle volume are always larger in *A. atropos*. Yet, in relation to the proximal and distal proboscis regions, lateral intrinsic muscle volume in the tip region of *A. atropos* is substantially smaller and and "only" twice as large as the lateral intrinsic muscle volume of *A. convolvuli*. This, as well as the absence of internal galea musculature in the apex of the proboscis tip, suggests that tip mobility and flexibility are reduced. Thus, the proboscis tip of *A. atropos* has probably been primarily selected for stability.

Muscle fibers are substantially longer in *A. atropos*, also when compared to other nectar feeders besides *A. convolvuli*. As an example, primary oblique muscles in *Vanessa cardui* (Linnaeus, 1758) are 250 – 300 µm long (Krenn 2000). The longest muscle fiber was measured in the proximal region of *A. atropos*. In *A. convolvuli*, the longest fiber was measured in the tip region of the galea, implementing a higher mobility of this region.

Most astoundingly, muscle volume extrapolated onto the entire proboscis length is considerably larger in *A. atropos*, although the proboscis is only about a fifth of the proboscis length of *A. convolvuli*. Longer muscle fibers and a larger internal galea muscle volume may be explainable by the stiffness and robust build of the piercing proboscis in *A. atropos*. As proboscis diameter, food canal diameter and cuticula width are all increased, a co-development of larger, more voluminous muscles was necessary to maintain proboscis movement.

The asymmetric arrangement of lateral and median intrinsic muscles in the tip region of the studied *A. atropos* specimen may be a structural adaptation or possibly an artefact caused by chemical fixation or other processes. An asymmetrical muscle arrangement in the tip region may enable differing movements of the individual galeae or a slight displacement of one galea relative to the other in this area. However, this has never been observed in *A. atropos*. As previously mentioned, the piercing mechanism is mainly enabled by shear force. It is further important to mention, that only one specimen was analyzed in this context. Therefore, it cannot be ruled out that the muscular arrangement at hand is exclusive to the studied individual.

4.2.3 External Galea Musculature

The basal galea musculature as well as the stipes musculature show a relatively uniform arrangement and very similar size proportions in *A. atropos* and *A. convolvuli*. This is rather

interesting considering that *A. atropos* can use structures of the proboscis base to produce sound (Brehm et al. 2015). The external and internal stipes muscles are only slightly larger in *A. convolvuli* while the basal galea muscle is slightly larger in *A. atropos*. The external stipes muscles are only involved in hydraulic uncoiling of the proboscis and are primarily responsible for increasing the hemolymph pressure inside the head cavity, which in turn forces hemolymph through the stipes valve into the galeae (Krenn 2010). This may suggest that the longer proboscis in the nectar feeder *A. convolvuli* requires a slightly larger muscular volume to generate a sufficient hemolymph pressure throughout the entire length of the proboscis. In turn, the internal stipes muscle is responsible for flexing the entire proboscis into resting position and not for movement of the proboscis while feeding (Krenn 2010). Again, the long proboscis in *A. convolvuli* may require a larger muscle for this movement. A larger basal galea muscle volume in *A. atropos* on the other hand, further supports the hypothesis that the robust nature of the galeae requires larger muscles for proboscis movement, such as the elevation of the proboscis. Still, external galea features are relatively similar in both species, even though they exhibit very different feeding preferences.

4.3 Advantages of Honey Feeding

But why does *A. atropos* drink honey in the first place? So far, there is no definitive answer. One possible hypothesis is that the higher sugar content of honey, compared to nectar, makes it a richer energy source. Therefore, *A. atropos* would take in more energy with little volume whereas nectar-feeders typically must continuously consume large quantities of nectar, which isn't as energy rich. This may enable *A. atropos* to go longer periods of time without consuming food, as it is known that this species migrates over long distances from Africa up north into parts of the palearctic region (Rothschild & Jordan 1903). Furthermore, not feeding on nectar may be a great advantage, especially outside of the vegetation period or in areas, which have non to little flower growth. However, many of the palearctic populations consist exclusively of individuals immigrating from the south during spring to late summer. These may reproduce, but mostly don´t survive the harsh winters in these regions (Rothschild & Jordan 1903; Ebert et al.1994). Offspring developing in Central-Europe is speculated to be mostly sterile and doesn´t migrate back to Africa during early autumn (Ebert et al. 1994), which in turn contributes to the line to dying out with the onset of winter. Until then, adults seem to survive by feeding on honey.

Conclusion

In *A. atropos*, the highly derived morphology of the proboscis, and especially of the proboscis tip, is just as unique as the moth´s lifestyle itself. In conjunction with the ability to drink honey, the death´s head hawkmoth displays a short and robustly built proboscis and an enlarged food canal diameter. To sustain the mobility of the galeae, *A. atropos* has enlarged intrinsic galea muscles. For piercing, the proboscis tip is sharply pointed and equipped with a large, subterminal opening of the food canal. This tip morphology is unique within the Lepidoptera. Therefore, the proboscis of *A. atropos* represents a new evolutionary solution for a piercing proboscis among lepidopterans. Extra-galeal features however, are similar to those of the nectar feeder *A. convolvuli*, implementing that the highly specialized feeding preference of *A. atropos* primarily selected for modifications of the proboscis. Accordingly, extra-galeal features are more conserved among these two species, as the functional mechanism of proboscis uncoiling and flexing may be more independent from modifications of the proboscis caused by distinct feeding preferences. Therefore, minor modifications occurred only in the size of the basal galea- and stipes muscles.

Phylogenetically, a short and pointed proboscis is considered a synapomorphy of all three *Acherontia* species (Kitching 2003). Furthermore, *Acherontia styx* (Westwood, 1847) and *Acherontia lachesis* (Fabricius, 1798) have also been recorded to raid beehives (Kitching 2003) and are able to produce sounds (Kitching 2003, personal observation). However, this has not been adequately investigated in these two species. Potential similarities in proboscis anatomy and tip morphology of all three species of the genus *Acherontia* are therefore yet to be determined and should be subject of future research.

References

Abdallah, A. I. A. A., 2014. Some Physicochemical Characteristics of Natural Bee Honey And Tow Commercial Types of Honey. Doctoral dissertation, University of Gezira, 1-43

Altner, H., Loftus, R., Schaller-Selzer, L., Tichy, H., 1983. Modality- specificity in insect sensilla and multimodal input from body appendages. Fortschritte der Zoologie Bd. 28: 17–31

Amsel, H. G., 1938. *Amphimoea walkeri* Bsd., der Schwärmer mit dem längsten Rüssel. Entomologische Rundschau, 55: 165-167

Bar-On, B., 2019. On the form and bio-mechanics of venom-injection elements. Acta biomaterialia, 85: 263-271

Bänziger, H., 1968. Preliminary observations on a skin-piercing blood-sucking moth (*Calyptra eustrigata* (Hmps.) (Lep., Noctuidae)) in Malaya. Bulletin of Entomological Research, 58: 159-163

Bänziger, H., 1970. The Piercing Mechanism of the Fruit-piercing Moth *Calpe* [Calyptra] *thalictri* bkh. (Noctuidae) with Reference to the Skin-piercing Blood-sucking Moth *C. eustrigata* hmps. Acta Tropica, 27: 54-88

Bänziger, H., 1971. Extension and coiling of the lepidopterous proboscis—a new interpretation of the blood-pressure theory. Mitt. Schweiz. Entomol. Ges, 43: 225-239

Bänziger, H., 1980. Skin-piercing blood-sucking moths. III: Feeding act and piercing mechanism of *Calyptra eustrigata* (Hmps.) (Lep., Noctuidae). Mitt. Schweiz. Entomol. Ges, 53: 127-142

Bauder, J. A. S., Handschuh, S., Metscher, B. D., Krenn, H. W., 2013. Functional morphology of the feeding apparatus and evolution of proboscis length in metalmark butterflies (Lepidoptera: Riodinidae). Biological Journal of the Linnean Society, 110: 291-304

Bauder, J. A., Lieskonig, N. R., Krenn, H. W., 2011. The extremely long-tongued Neotropical butterfly *Eurybia lycisca* (Riodinidae): proboscis morphology and flower handling. Arthropod Structure & Development, 40: 122-127

Blaney, W. M., Simmonds, M. S. J., 1988. Food selection in adults and larvae of three species of Lepidoptera: a behavioural and electrophysiological study. Entomologia Experimentalis et Applicata, 49: 111–121

Bock, C., 1987. A quick and simple method of preparing soft insect tissues for scanning electron microscopy using carnoy and hexamethyldisilazane. Beitr. Elektronenmikrosk. Direktabb. Oberfl., 20: 209-214

Brehm, G., Fischer, M., Gorb, S., Kleinteich, T., Kühn, B., Neubert, D., Pohl, H., Wipfler, B., Wurdinger, S., 2015. The unique sound production of the Death's-head hawkmoth (*Acherontia atropos* (Linnaeus, 1758)) revisited. The Science of Nature, 102: 1-13

Büttiker, W., Krenn, H. W., Putterill, J. F., 1996. The proboscis of eye-frequenting and piercing Lepidoptera (Insecta). Zoomorphology, 116: 77-83

Du Plessis, A., Broeckhoven, C., Le Roux, S. G., 2018. Snake fangs: 3D morphological and mechanical analysis by microCT, simulation, and physical compression testing. Gigascience, 7: 1-8

Eastham, L. E. S., Eassa, Y. E. E., 1955. The feeding mechanism of the butterfly *Pieris brassicae* L. Philosophical Transactions of the Royal Society of London. Series B, Biological Sciences, 239: 1-43

Ebert, G., Hirneisen, N., Krell, F. T., 1994. Die Schmetterlinge Baden-Württembergs, Nachtfalter II. Eugen Ulmer Verlag, Band 4

Eyer, M., Neumann, P., Dietemann, V., 2016. A look into the cell: honey storage in honey bees, *Apis mellifera*. PloS one, 11: 1-20

Faucheux, M. J., 2007. L'apparition des sensilles styloconiques sur la trompe au cours de l'évolution des Lépidoptères: Les pièces buccales d'*Apoplania valdiviana* Davis & Nielsen 1984 (Glossata: Neopseustoidea): Neopseustidae). Bulletin de la Société des Sciences Naturelles de l'Ouest de la France, 29: 206–217

Faucheux, M. J., 2013. Sensillum types on the proboscis of the Lepidoptera: a review. In Annales de la Société entomologique de France, 49: 73-90

Foelix, R.F., 2011. Biology of spiders. OUP USA. third edition: 21-22

Garcia, J. M., Chambers, E., Matta, Z., Clark, M., 2005. Viscosity measurements of nectar- and honey-thick liquids: product, liquid, and time comparisons. Dysphagia, 20: 325-335

Gnatzy W., Tautz J., 1980. Ultrastructure and mechanical properties of an insect mechanoreceptor: Stimulus-transmitting structures and sensory apparatus of the cercal filiform hairs of *Gryllus*. Cell and Tissue Research, 213: 441-463

Haber, W. A., Frankie, G. W., 1989. A Tropical Hawkmoth Community: Costa Rican Dry Forest Sphingidae. Biotropica, 21: 155-172

Huber, R. L., 1946. U.S. Patent No. 2,409,979. Washington, DC: U.S. Patent and Trademark Office: 1-4

Hüsing, J. O., Nitschmann, J., 1987. Lexikon der Bienenkunde. Ehrenwirth Verlag.

Kitching I. J., 2003. Phylogeny of the death ´s head hawkmoths, *Acherontia* [Laspeyres], and related genera (Lepidoptera: Sphingidae: Sphinginae: Acherontiini). Systematic Entomology 28: 71-88

Kornev, K. G., Salamatin, A. A., Adler, P. H., Beard, C. E., 2017. Structural and physical determinants of the proboscis–sucking pump complex in the evolution of fluid-feeding insects. Scientific reports, 7: 1-18

Krenn, H. W., 1990. Functional morphology and movement of the proboscis of Lepidoptera (Insecta). Zoomorphology 110: 105-114

Krenn, H. W., 1998. Proboscis sensilla in *Vanessa cardui* (Nymphalidae, Lepidoptera): functional morphology and significance in flower-probing. Zoomorphology, 118: 23-30

Krenn, H. W., 2000. Proboscis musculature in the butterfly *Vanessa cardui* (Nymphalidae, Lepidoptera): settling the proboscis recoiling controversy. Acta Zoologica, 81: 259-266

Krenn, H. W., 2008. Feeding behaviours of neotropical butterflies (Lepidoptera, Papilionoidea). Denisia, zugleich Kataloge der oberösterreichischen Landesmuseen Neue Serie, 88: 295-304

Krenn, H.W., 2010. Feeding Mechanisms of Adult Lepidoptera: Structure, Function, and Evolution of the Mouthparts. Annu. Rev. Entomol. 55: 307–27

Krenn, H. W., Aspöck, H., 2012. Form, function and evolution of the mouthparts of blood-feeding Arthropoda. Arthropod structure & development, 41: 101-118

Krenn, H. W., Bauder, J. A. S., 2018. Morphological fine tuning of the feeding apparatus to proboscis length in Hesperiidae (Lepidoptera). Journal of morphology, 279: 396-408

Krenn, H.W., Kristensen, N.P., 2000. Early evolution of the proboscis of Lepidoptera (Insecta): external morphology of the galea in basal glossatan moth lineages, with remarks on the origin of the pilifers. Zoologischer Anzeiger, 239: 179–196

Krenn, H. W., Kristensen, N. P., 2004. Evolution of proboscis musculature in Lepidoptera. European Journal of Entomology, 101: 565-575

Krenn, H.W., Mühlberger, N., 2002. Groundplan Anatomy of the Proboscis of Butterflies (Papilionoidea, Lepidoptera). Zoologischer Anzeiger, 241: 369–380

Krenn, H. W., Zulka, K. P., Gatschnegg, T., 2001. Proboscis morphology and food preferences in nymphalid butterflies (Lepidoptera: Nymphalidae). Journal of Zoology, 254: 17-26

Kridi, D. S., Carvalho, C. G. N. D., Gomes, D. G., 2014. A Predictive Algorithm for Mitigate Swarming Bees through Proactive Monitoring via Wireless Sensor Networks. In Proceedings of the 11th ACM symposium on Performance evaluation of wireless ad hoc, sensor, & ubiquitous networks, 41-47

Lehnert M. S., Beard, C.E., Gerard, P.D., Kornev, K.G., Adler, P.H., 2016. Structure of the Lepidopteran Proboscis in Relation to Feeding Guild. Journal of Morphology, 277: 167–182

Lehnert, M. S., Monaenkova, D., Andrukh, T., Beard, C. E., Adler, P. H., Kornev, K. G. 2013. Hydrophobic–hydrophilic dichotomy of the butterfly proboscis. Journal of the Royal Society Interface, 10: 1-10

Lipp, J., 1994. Handbuch der Bienenkunde. Der Honig. Eugen Ulmer Verlag, Band 3

Ma, L., Hu, K., Li, P., Liu, J., Yuan, X., 2019. Ultrastructure of the proboscis sensilla of ten species of butterflies (Insecta: Lepidoptera). PloS one, 14: 1-13

Misof, B., Liu, S., Meusemann, K., Peters, R. S., Donath, A., Mayer, C., et al., 2014. Phylogenomics resolves the timing and pattern of insect evolution. Science 346.6210: 763-767

Mitter, C., Davis, D. R., Cummings, M. P., 2017. Phylogeny and Evolution of Lepidoptera. Annu. Rev. Entomol., 62: 265–83

Moritz, R. A., Kirchner W. H., Crewe R. M., 1991. Chemical Camouflage of the Death ´s Head Hawkmoth (*Acherontia atropos* L.) in Honeybee Colonies. Naturwissenschaften, 78: 179-182

Naheed, R., Farooqi, S. R., 2018. Physical characterization and antibiotic potential of honey collected from *A. florea* combs in district Khairpur. Journal of Entomology and Zoology Studies, 6: 1564-1570

Netz, C., Renner, S. S., 2017. Long-spurred *Angraecum* orchids and long-tongued sphingid moths on Madagascar: a time frame for Darwin's predicted *Xanthopan/Angraecum* coevolution. Biological Journal of the Linnean Society, 122: 469-478

Nilsson, L. A., Jonsson, L., Rason, L., Randrianjohany, E., 1985. Monophily and pollinationmechanisms in *Angraecum arachnites Schltr*. (Orchidaceae) in a guild of long-tongued hawk-moths (Sphingidae) in Madagascar. Biological Journal of the Linnean Society, 26: 1-19

Oroian, M., 2013. Measurement, prediction and correlation of density, viscosity, surface tension and ultrasonic velocity of different honey types at different temperatures. Journal of Food Engineering, 119: 167-172

Park, O. W., 1933. Studies on the rate at which honeybees ripen honey. Journal of Economic Entomology, 26: 188-193

Petr, D., Stewart, K. W., 2004. Comparative morphology of sensilla styloconica on the proboscis of North American Nymphalidae and other selected taxa (Lepidoptera): systematic and ecological considerations. Transactions of the American Entomological Society, 130: 293-409

Pinterich, E., Krenn, H. W., 2020. Fruit-feeding behavior of the butterfly *Consul fabius* (Charaxinae, Nymphalidae, Lepidoptera). Entomologica Austriaca, 27: 91-105

Plotkin, D., Goddard, J., 2013. Blood, sweat, and tears: a review of the hematophagous, sudophagous, and lachryphagous Lepidoptera. Journal of Vector Ecology, 38: 289-294

Powell, J. A., 2009. Lepidoptera: moths, butterflies. In Encyclopedia of insects. Academic Press. Second Edition: 559-587

Rothschild, L. W. R. B., Jordan, K., 1903. A revision of the lepidopterous family Sphingidae. Hazell, Watson & Viney, Ld., 1: 162-163

Salama, H. S., Khalifa, A., Azmy, N., Sharaby, A., 1984. Gustation in the lepidopteran moth *Spodoptera littoralis* (Boisd.). Zoologische Jahrbücher Physiologie, 88: 165–178

Smola, T., 2021. Morphologie des Rüssels der Sphingidae: Sensillen und Länge der apikalen Region. Bachelor-thesis. University of Vienna, 1-33

Stöckl, A. L., Kelber, A., 2019. Fuelling on the wing: sensory ecology of hawkmoth foraging. Journal of Comparative Physiology A, 205: 399-413

Wannenmacher, G., Wasserthal, L. T., 2003. Contribution of the maxillary muscles to proboscis movement in hawkmoths (Lepidoptera: Sphingidae)—an electrophysiological study. Journal of Insect Physiology, 49: 765-776

Wasserthal, L. T., 1997. The pollinators of the Malagasy star orchids *Angraecum sesquipedale*, *A. sororium* and *A. compactum* and the evolution of extremely long spurs by pollinator shift. Botanica Acta, 110: 343-359

Zaspel, J. M., 2008. Systematics, biology, and behavior of fruit-piercing and blood-feeding moths in the subfamily Calpinae (Lepidoptera: Noctuidae). Dissertation. University of Florida, 1-190

Zaspel, J. M., Weller, S. J., Branham, M. A., 2011. A comparative survey of proboscis morphology and associated structures in fruit-piercing, tear-feeding, and blood-feeding moths in Calpinae (Lepidoptera: Erebidae). Zoomorphology, 130: 203-225

Zenker, M. M., Penz, C., De Paris, M., Specht, A., 2011. Proboscis morphology and its relationship to feeding habits in noctuid moths. Journal of Insect Science. 11: 1-10

Zhao, Z. L., Shu, T., Feng, X. Q., 2016. Study of biomechanical, anatomical, and physiological properties of scorpion stingers for developing biomimetic materials. Materials Science and Engineering: C, 58: 1112-1121

Appendix

Zusammenfassung

Innerhalb der Lepidoptera treten oftmals verschiedene Rüsselmorphologien im Zusammenhang mit unterschiedlichen Nahrungsgilden auf. Besonders der Totenkopfschwärmer, *Acherontia atropos* (Linnaues, 1758), weist eine hoch spezialisierte Form des Nahrungserwerbs auf. Im Gegensatz zu Blütenbesuchern, ist diese Art dafür bekannt, mithilfe ihres Rüssels Honigwaben zu durchstechen und den enthaltenen Honig aufzusaugen. Dieses außergewöhnliche Verhalten hat bereits zahlreiche Untersuchungen der verschiedenen Anpassungen dieser Art, wie chemische Tarnung oder die Anatomie des Rüssels in Bezug auf Lautäußerung, nach sich gezogen. Die detaillierte Erfassung der Anpassungen des Rüssels und der Stipespumpe im Hinblick auf die Nahrungsaufnahme dieser Art, wurde jedoch in der Vergangenheit stark vernachlässigt. Daher wurden im Zuge dieser Studie mittels serieller Semidünnschnitte, MicroCT-Scans sowie der REM-Bildgebung, morphologische und anatomische Analysen des Rüssels und der Stipespumpe durchgeführt. Die Merkmale von *A. atropos* wurden mit *Agrius convolvuli* (Linnaeus, 1758), einer verwandten, Nektar saugenden Art, verglichen. Die Ergebnisse unterstreichen eine einzigartige Morphologie des kurzen, spitzen Rüssels in *A. atropos*. Die große Öffnung des Nahrungskanals ist elliptisch und subterminal positioniert – eine Anpassung, die Stabilität bieten und zugleich auch Verstopfungen vorbeugen soll. Anatomisch weisen beide Arten denselben Grundbauplan der internen Galea Muskulatur, des basalen Galea Muskels und der Stipes Muskeln auf. Dennoch übersteigt das Volumen der internen Galea Muskulatur von *A. atropos* bei weitem das Volumen der internen Galea Muskulatur bei *A. convolvuli*. Das Volumen der Stipes Muskulatur und des basalen Galea Muskels hingegen ist bei beiden Arten ähnlich. All dies deutet darauf hin, das gewisse Teile des Nahrungsapparats, wie etwa der Rüssel, beim Totenkopfschwärmer hoch spezialisiert sind, während besonders der Grundbauplan extra-galealer Strukturen bei beiden Arten stärker konserviert sein dürfte.